Space-Time Trefftz - Discontinuous Galerkin Approximation for Elasto-Acoustics

Hélène Barucq, Henri Calandra, Julien Diaz, Elvira Shishenina

Space-Time Trefftz - Discontinuous Galerkin Approximation for Elasto-Acoustics

Hélène Barucq, Henri Calandra, Julien Diaz, Elvira Shishenina

RESEARCH REPORT
N° 9104
October 2017
Project-Team Magique-3D

ISSN 0249-6399 ISRN INRIA/RR--9104--FR+ENG

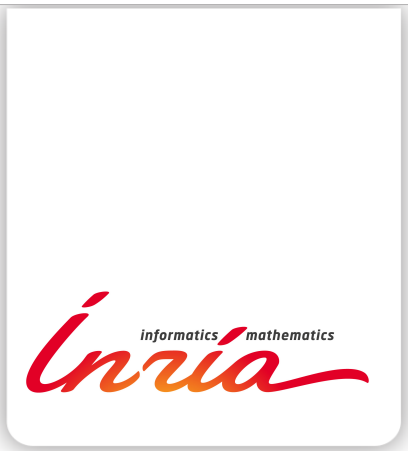

Space-Time Trefftz - Discontinuous Galerkin Approximation for Elasto-Acoustics

Hélène Barucq*, Henri Calandra†, Julien Diaz*, Elvira Shishenina*†

Project-Team Magique-3D

Research Report n° 9104 — October 2017 — 43 pages

This work is supported by the collaborative research program Depth Imaging Partnership between team-project Magique-3D of Inria, Bordeaux-Sud-Ouest, and Prospective Lab of Total S.A., Houston.

* Inria, UPPA-CNRS, France
† Total S.A., USA

RESEARCH CENTRE
BORDEAUX – SUD-OUEST

200 avenue de la Vieille Tour
33405 Talence Cedex

Abstract: Wave reflection imaging for complex media can be effectively done by using advanced numerical methods (see [19]). In the context of the collaborative research program Depth Imaging Partnership (DIP) between Inria and Total, team-project Magique-3D and Prospective Lab of Houston develop high-order numerical schemes based mostly on discontinuous finite element approximation of wave fields. This technique, known as Discontinuous Galerkin (DG) method, is preferred because it takes into account geometrical and physical features of environment, and it is well-adapted for parallel computation [4, 19]. Recently it has been implemented for coupled elasto-acoustic problems, which led to the development of new propagators in time and frequency domains [6, 34].
However, when comparing to the conventional methods based on continuous approximation, the number of degrees of freedom required by DG method to achieve the same accuracy is significantly higher.
To avoid this difficulty, Hybridizable Discontinuous Galerkin (HDG) methods have been developed and their integration into DIP is under way for both acoustic and elastic domains, with possibility of numerical coupling (see [22] and references therein).
Another idea to explore consists in using Trefftz approximation space, whose elements are themselves discrete local solutions of the Acoustic System (AS) and Elastodynamic System (ES) [18, 32]. By its construction, Trefftz method reduces degrees of freedom, since it requires computing the surface integrals only to build variational formulation. Thus, we may consider the following advantages of Trefftz method compared to the standard ones: better order of convergence, flexibility in the choice of basis functions, low dispersion, incorporation of wave propagation directions in the discrete space, adaptivity and local space-time mesh refinement [18, 32].
Trefftz type methods have been widely used with time-harmonic formulations by Farhat, Tezaur, Harari, Hetmaniuk (2003 - 2006) (see [15, 31]), Gabard (2007) (see [17]), Badics (2014) (see [3]), Hiptmair, Moiola, Perugia (2011 - 2013) (see [20, 21, 28]) and others, while studies are still limited for reproducing temporal phenomena. Only few papers are interested in Maxwell equations in time [14, 23, 24, 30], but they are mostly devoted to a theoretical analysis of the method, showing the convergence and stability, and numerical tests with plane waves approximation are restricted to 1D + time dimensional case.
Space-time Trefftz approximation by Lagrange multipliers for the second order formulation of the transient wave equation was explored in [5, 33].
Trefftz - Discontinuous Galerkin (Trefftz-DG) method for the first-order transient acoustic wave equations in arbitrary space dimensions extending the one-dimensional scheme of Kretzschmar et al. [23] has been introduced in recent paper of Moiola and Perugia (2017) [29]. the authors propose a complete a priori error analysis in both mesh-dependent and mesh-independent norms.
In order to move on numerical simulations of geophysical phenomena and to consider more realistic application, DIP aims to develop new approximation techniques, which retain DG based methods but operates the Trefftz approach.

Key-words: Trefftz approximation, space-time mesh, Trefftz-DG formulation, elasto-acoustic system

Approximation Espace-Temps de Trefftz - Galerkin Discontinue pour l'Élasto-Acoustique

Résumé : L'imagerie de milieux complexes par réflexion d'ondes peut se faire de manière efficace en utilisant des méthodes numériques avancées. Dans le contexte du programme de recherche collaborative DIP liant Inria et Total, l'équipe Magique-3D développe avec le Prospective Lab de Houston des schémas d'ordre élevé, essentiellement basés sur des approximations discontinues par éléments finis des champs d'ondes. Cette technique, connue sous le nom de méthode DG est privilégiée car elle permet de tenir compte des caractéristiques géometriques et physiques du milieu et qu'elle est adaptée au calcul parallèle [4, 19]. Récemment, elle a été mise en oeuvre pour des problèmes couplés d'élasto-acoustique, ce qui a donné lieu au développement des nouveax propagateurs dans le domaine temporel et le domaine harmonique [6, 34].

Si les méthodes d'éléments finis discontinus ont fait leurs preuves en matière de précision et de flexibilité, elles sont critiquées pour le nombre de degrés de liberté qu'elles utilisent qui s'avère beaucoup plus élevé que les méthodes classiques basées sur des approximations continues.

Pour surmonter cette difficulté, des méthodes hybrides dites "Hybridizable Discontinuous Galerkin methods" ont été développées et leur intégration dans le projet DIP est en cours, aussi bien dans le domaine acoustique qu'élastique (voir [22]).

Une autre idée consiste à utiliser des méthodes de Trefftz pour lesquelles on utilise des espaces discrets dont les éléments sont des solutions locales des équations à résoudre.

Cette approche a été souvent utilisée pour résoudre des équations d'ondes harmoniques par Farhat, Tezaur, Harari, Hetmaniuk (2003 - 2006) (voir [15, 31]), Gabard (2007) (voir [17]), Badics (2014) (voir [3]), Hiptmair, Moiola, Perugia (2011 - 2013) (voir [20, 21, 28]) et les autres, mais très peu pour reproduire des phénomènes temporels. Quelques articles récents de 2014-2017 [14, 23, 24, 29, 30] s'intéressent aux équations temporelles de Maxwell mais l'essentiel des papiers se consacre à l'analyse théorique de la méthode, démontrant la convergence et stabilité.

Dans le but de continuer à faire évoluer son expertise dans le domaine de la simulation numérique de phénomènes géophysiques, le projet DIP souhaite développer de nouvelles techniques d'approximation qui conservent pour socle les méthodes DG mais qui exploitent de Trefftz approche dans le but de considérer des applications de plus en plus réalistes.

Mots-clés : approximation de Trefftz, couplage élasto-acoustique, maillage espace-temps, méthode des elements finis discontinues

1 Introduction

In this Chapter we give an introduction to a seismic data acquisition and processing. We compare some advanced and widely used numerical methods, and we give a general motivation for the further studies.

1.1 Seismic survey

Systematic collection and analysis of geophysical data is called geophysical survey. Geophysical signal transmitted into the Earth interior is the main tool used by geophysicists. Detection and analysis of these signals are the core parts of geophysical signal processing. In industrial applications they permit a fine mapping of the Earth structure and serve as a milestone of the search for natural resources, such as oil, gas, or minerals.

The main form of geophysical survey is the seismic survey. This method is in fact very close to the ultrasound techniques used in medicine and in a number of other applications. The sources of pressure waves can be different, depending on the surrounding media: for example, compressed air in fluid, and vibrator, or explosive in solid media. Created waves are reflected at the interfaces between media layers with different geological properties and recorded by a grid of on-surface sensors - receiver array. The acquired data are subject to numerical analysis, that converts them into a seismic image. This image can be two, three, or four dimensional (in the latest case the fourth dimension traces fluid distribution as a function of survey data) [1, 13].

This processing and analysis requires not only a big computational power, but also a very sophisticated software that combines the current knowledge in mathematics, physics and numerical methods.

1.2 Basic numerical methods

Modern computing efficiency increased to a state where we can compute wave field simulations for realistic 3D models with frequencies of interest of seismologists and engineers. Nevertheless, at this stage it is still important to have a good mathematical interpretation of physical mechanism. A proper method will not only improve a modelling accuracy, but also would give a better mastery in the characterization of the mechanism itself.

Currently, the most popular numerical methods are the grid-based techniques, which interpolate the wave field on a grid of 3D points, for example: Finite Difference Method (FDM), Finite Volume Method (FVM), Finite Element Method (FEM) and Spectral Element Method (SEM) [19]. In general, the main differences between the methods lay in the way they represent the exact solution by an approximate one, and in the way this approximate solution satisfies the Partial Differential Equation (PDE). The most widely known FDM, FEM and FVM are all techniques used to derive discrete representation of the spatial derivative operators. Moreover, when adding a time variable, we can address a wide variety of methods for integrating the ordinary differential equations [19].

Some general properties of these methods and their advantages and drawbacks with respect to the different numerical criteria are given in Table 1. Here, "+" represents success, "−" indicates a weakness in the method, and "(+)" reflects that the method with modifications is capable of solving such problems but remains a less natural choice [19].

Trefftz-DG methods consist in a special choice of basis function, which represent themselves the exact local solutions of the initial equations. It vanishes all volume integral terms in a final variational formulation, and reduce the number of equations, as they have to be formed only at the boundaries. For time dependent problems it requires space-time mesh. Thus, all the

Numerical method	Complex geometries	High-order accuracy and *hp*-adaptivity	Explicit semi-discrete form	Conservation laws	Elliptic problems
FDM	-	+	+	+	+
FVM	+	-	+	+	(+)
FEM	+	+	-	(+)	+
DG-FEM	+	+	+	+	(+)

Table 1: Generic properties of the most widely used numerical methods [19]

algebraic equations are coupled and matrices are full as the test functions will need to be defined over the whole domain [16].

In Chapter 2, we develop a theory for Trefftz-DG method applied to the Acoustic System (AS), Elastodynamic System (ES), and, by introducing the fluid-solid transmission conditions, for coupled Elasto-Acoustic System (EAS). We study well-posedness of each problem, and prove a priori error estimates in mesh dependent norms. In Chapter 3, we consider a space-time polynomial basis, and we develop the algorithm of implementation of the method for 1D example of AS. Some numerical results for 2D AS, ES, and coupled EAS are given in Chapter 4. We give a short conclusion and discuss the perspectives in the end of this report.

2 Trefftz method: theory and application to the elasto-acoustics

In this Chapter we apply Trefftz-DG method for solving first-order Acoustic and Elastodynamic systems. Then, we couple numerically two formulations by introducing the transmission conditions. We provide studies of well-posedness of each problem.

2.1 Application to acoustics

We introduce first order AS and build a discrete DG formulation. Then, we introduce the Trefftz space and develop a coupled Trefftz-DG formulation for initial acoustic problem. We also provide the analysis of well-posedness of final Trefftz-DG formulation, based on the coercivity and continuity estimates in mesh-dependent norms (here and further the subscript F corresponds to "Fluid" - acoustic medium indicator).

2.1.1 Acoustic system

To consider an Initial Boundary Value Problem (IBVP) in fluid media, we introduce a global space-time domain $Q_F \equiv \Omega_F \times I$, where $\Omega_F \subset R^n$ - a bounded Lipschitz space domain, and a time interval $I \equiv [0, T]$.

We set fluid parameters $c_F \equiv c_F(x)$ and $\rho_F \equiv \rho_F(x)$, acoustic wave propagation velocity and fluid density respectively, piecewise constant and positive.

We consider first order AS in terms of velocity $v_F \equiv v_F(x,t)$ and pressure $p \equiv p(x,t)$ fields:

$$\begin{cases} \dfrac{1}{c_F^2 \rho_F}\dfrac{\partial p}{\partial t} + \mathrm{div} v_F = f \text{ in } Q_F, \\ \rho_F \dfrac{\partial v_F}{\partial t} + \nabla p = 0 \text{ in } Q_F, \\ v_F(\cdot, 0) = v_{F0},\ p(\cdot, 0) = p_0 \text{ in } \Omega_F, \\ v_F = \mathrm{g}_{D_F} \text{ in } \partial\Omega_F \times I, \end{cases} \tag{1}$$

The source function is represented by $f \equiv f(x,t)$, the boundary condition function by $\mathrm{g}_{D_F} \equiv \mathrm{g}_{D_F}(x,t)$, and the velocity v_{F0} and pressure p_0 are the initial data (further, the Dirichlet conditions on $\partial\Omega_F$ will be imposed).

2.1.2 Space-time DG formulation

Let $K_F \subset Q_F$, and $n_{K_F} \equiv (n^x_{K_F}, n^t_{K_F})$ - outward pointing unit normal vector on ∂K_F. Fluid parameters c_F, ρ_F are constant in K_F. Unknowns v_F and p are supposed to be in $H^1(K_F)$.

Multiplying both equations of (1) by the test functions q and $\omega_F \in H^1(K_F)$ respectively, and integrating two times by part in time and space, we obtain:

$$\begin{aligned} &-\int_{K_F} \Big[p\big(\frac{1}{c_F^2\rho_F}\frac{\partial q}{\partial t} + \mathrm{div}\omega_F\big) + v_F \cdot \big(\rho_F \frac{\partial \omega_F}{\partial t} + \nabla q\big)\Big] d\mathrm{v} \\ &+\int_{\partial K_F} \Big[\frac{1}{c_F^2\rho_F} p n^t_{K_F} q + v_F \cdot n^x_{K_F} q + \rho_F v_F n^t_{K_F} \cdot \omega_F + p n^x_{K_F} \cdot \omega_F \Big] d\mathrm{s} = \int_{K_F} f q d\mathrm{v}. \end{aligned} \tag{2}$$

To build a DG formulation, we introduce a non-overlapping mesh $\mathcal{T}_h \equiv \{K_F\}$ on Q_F.

Without losing generality with respect to the classical space DG methods, we start with particular cases of mesh, whose elements are right prisms, with vertical sides parallel to time axis. All fluid parameters inside the elements K_F are supposed to be constant, so that all discontinuities lie on the inter-element boundaries.

Since the space-time mesh has been introduced, the mesh skeleton $\mathcal{F}_h = \cup_{K_F \in \mathcal{T}_h} \partial K_F$ can be decomposed into families of element faces as follows [23]:

$$\begin{aligned}
\mathcal{F}_h^{\Omega_F} &- \text{ internal } \Omega\text{-faces } (t \text{ - fixed}),\\
\mathcal{F}_h^{I_F} &- \text{ internal } I\text{-faces } (x \text{ - fixed}),\\
\mathcal{F}_h^{0_F} &- \text{ external initial time faces } (\Omega_F \times \{0\}),\\
\mathcal{F}_h^{T_F} &- \text{ external final time faces } (\Omega_F \times \{T\}),\\
\mathcal{F}_h^{D_F} &- \text{ external Dirichlet boundary faces } (\partial\Omega_F \times [0,T]).
\end{aligned}$$

To fix notations in the standard DG terms, we define the averages $\{\cdot\}$, space normal jumps $[\![\cdot]\!]_x$ and time jumps $[\![\cdot]\!]_t$ between two elements K_F^1, K_F^2 for piecewise-continuous scalar p and vector v_F fields [19]:

$$\begin{aligned}
\{p\} &\equiv \frac{1}{2}(p_{|K_F^1} + p_{|K_F^2}) && \text{on } \partial K_F^1 \cap \partial K_F^2 \subset \mathcal{F}_h^{I_F},\\
[\![p]\!]_x &\equiv p_{|K_F^1} n^x_{K_F^1} + p_{|K_F^2} n^x_{K_F^2} && \text{on } \partial K_F^1 \cap \partial K_F^2 \subset \mathcal{F}_h^{I_F},\\
[\![p]\!]_t &\equiv p_{|K_F^1} n^t_{K_F^1} + p_{|K_F^2} n^t_{K_F^2} && \text{on } \partial K_F^1 \cap \partial K_F^2 \subset \mathcal{F}_h^{\Omega_F},\\
\{v_F\} &\equiv \frac{1}{2}(v_{F|K_F^1} + v_{F|K_F^2}) && \text{on } \partial K_F^1 \cap \partial K_F^2 \subset \mathcal{F}_h^{I_F},\\
[\![v_F]\!]_x &\equiv v_{F|K_F^1} \cdot n^x_{K_F^1} + v_{F|K_F^2} \cdot n^x_{K_F^2} && \text{on } \partial K_F^1 \cap \partial K_F^2 \subset \mathcal{F}_h^{I_F},\\
[\![v_F]\!]_t &\equiv v_{F|K_F^1} n^t_{K_F^1} + v_{F|K_F^2} n^t_{K_F^2} && \text{on } \partial K_F^1 \cap \partial K_F^2 \subset \mathcal{F}_h^{\Omega_F}.
\end{aligned}$$

We also use the superscripts "$-$" and "$+$" to refer to the interior and the exterior information respectively for each element [19].

The space-time DG formulation of the IBVP consists in searching $(v_{Fh}, p_h) \subset \mathbf{V}(\mathcal{T}_h) \subset H^1(\mathcal{T}_h)^2$ such that, for all $K_F \in \mathcal{T}_h$ and for all $(\omega_F, q) \subset \mathbf{V}(\mathcal{T}_h)$, it holds true:

$$\begin{aligned}
&-\int_{K_F} \Big[p_h\big(\frac{1}{c_F^2\rho_F}\frac{\partial q}{\partial t} + \mathrm{div}\omega_F\big) + v_{Fh}\cdot\big(\rho_F\frac{\partial \omega_F}{\partial t} + \nabla q\big)\Big]d\mathrm{v}\\
&+\int_{\partial K_F}\Big[\frac{1}{c_F^2\rho_F}\hat{p_h}n^t_{K_F}q + v_{\hat{F}h}\cdot n^x_{K_F}q + \rho_F v_{\hat{F}h}n^t_{K_F}\cdot\omega_F + \hat{p_h}n^x_{K_F}\cdot\omega_F\Big]d\mathrm{s} = \int_{K_F} fq d\mathrm{v}.
\end{aligned} \tag{3}$$

The numerical fluxes $v_{\hat{F}h}$, $\hat{p_h}$ on the mesh skeleton $\mathcal{F}_h$ are defined as follows:

$$\begin{aligned}
\begin{pmatrix} v_{\hat{F}h} \\ \hat{p_h}\end{pmatrix} &\equiv \begin{pmatrix} \{v_{Fh}\} + \beta[\![p_h]\!]_x \\ \{p_h\} + \alpha[\![v_{Fh}]\!]_x\end{pmatrix} && \text{on } \mathcal{F}_h^{I_F},\\
\begin{pmatrix} v_{\hat{F}h}\cdot n^x_{K_F} \\ \hat{p_h}n^x_{K_F}\end{pmatrix} &\equiv \begin{pmatrix} \mathrm{g}_{D_F}\cdot n^x_{K_F} \\ p_h n^x_{K_F} + \alpha(v_{Fh} - \mathrm{g}_{D_F})\cdot n^x_{K_F}\end{pmatrix} && \text{on } \mathcal{F}_h^{D_F},\\
\begin{pmatrix} v_{\hat{F}h} \\ \hat{p_h}\end{pmatrix} &\equiv \begin{pmatrix} {v_{Fh}}^- \\ {p_h}^-\end{pmatrix} && \text{on } \mathcal{F}_h^{\Omega_F},
\end{aligned}$$

$$\begin{pmatrix} v_{\hat{F}h} \\ \hat{p_h} \end{pmatrix} \equiv \begin{pmatrix} v_{Fh} \\ p_h \end{pmatrix} \quad \text{on } \mathcal{F}_h^{T_F},$$
$$\begin{pmatrix} v_{\hat{F}h} \\ \hat{p_h} \end{pmatrix} \equiv \begin{pmatrix} v_{F0} \\ p_0 \end{pmatrix} \quad \text{on } \mathcal{F}_h^{0_F}.$$

Here $\alpha \in L^\infty(\mathcal{F}_h^{I_F} \cup \mathcal{F}_h^{D_F})$ and $\beta \in L^\infty(\mathcal{F}_h^{I_F})$ are positive flux parameters [23]. Other choices of penalty terms are possible in order to achieve numerical stability of the scheme [2, 7, 8, 10].

Summing (3) over all elements $K_F \in \mathcal{T}_h$, we obtain DG formulation for (1):

Seek $(v_{Fh}, p_h) \subset \mathbf{V}(\mathcal{T}_h)$ *such that, for all* $(\omega_F, q) \subset \mathbf{V}(\mathcal{T}_h)$, *it holds:*

$$\begin{aligned}
\sum_{K_F \in \mathcal{T}_h} & -\int_{K_F} \Big[p_h \big(\frac{1}{c_F^2 \rho_F} \frac{\partial q}{\partial t} + \mathrm{div}\omega_F\big) + v_{Fh}\big(\rho_F \frac{\partial \omega_F}{\partial t} + \nabla q\big)\Big] d\mathrm{v} \\
& + \int_{\mathcal{F}_h^{\Omega_F}} \Big[\frac{1}{c_F^2 \rho_F} p_h{}^- [\![q]\!]_t + \rho_F v_{Fh}{}^- [\![\omega_F]\!]_t\Big] d\mathrm{s} \\
& + \int_{\mathcal{F}_h^{I_F}} \Big[\{\!\{p_h\}\!\} [\![\omega_F]\!]_x + \{\!\{v_{Fh}\}\!\} [\![q]\!]_x + \alpha [\![v_{Fh}]\!]_x [\![\omega_F]\!]_x + \beta [\![p_h]\!]_x [\![q]\!]_x \Big] d\mathrm{s} \\
& + \int_{\mathcal{F}_h^{T_F}} \Big[\frac{1}{c_F^2 \rho_F} p_h q + \rho_F v_{Fh} \cdot \omega_F\Big] d\mathrm{s} - \frac{1}{2} \int_{\mathcal{F}_h^{0_F}} \Big[\frac{1}{c_F^2 \rho_F} p_h q + \rho_F v_{Fh} \cdot \omega_F\Big] d\mathrm{s} \\
& + \int_{\mathcal{F}_h^{D_F}} \Big[p n_{K_F}^x \cdot \omega_F + \alpha v_{Fh} \cdot \omega_F\Big] d\mathrm{s} = \frac{1}{2} \int_{\mathcal{F}_h^{0_F}} \Big[\frac{1}{c_F^2 \rho_F} p_h q + \rho_F v_{Fh} \cdot \omega_F\Big] d\mathrm{s} \\
& + \int_{\mathcal{F}_h^{D_F}} \Big[\alpha \mathrm{g}_{D_F} \cdot \omega_F - \mathrm{g}_{D_F} \cdot n_{K_F}^x q\Big] d\mathrm{s} + \int_{K_F} f q d\mathrm{v}.
\end{aligned} \tag{4}$$

In the following, we will restrict the problem to the homogeneous system of equations with zero source $f \equiv 0$.

2.1.3 Trefftz-DG formulation

We define the Trefftz space:

$$\mathbf{T}_F(\mathcal{T}_h) \equiv \Big\{ (\omega_F, q) \subset H^1(\mathcal{T}_h)^2 \text{ s. t. } \rho_F \frac{\partial \omega_F}{\partial t} + \nabla q = \frac{1}{c_F^2 \rho_F} \frac{\partial q}{\partial t} + \mathrm{div}\omega_F = 0 \text{ in all } K_F \in \mathcal{T}_h \Big\}.$$

This choice of the discrete space $\mathbf{V}(\mathcal{T}_h)$ in $\mathbf{T}_F(\mathcal{T}_h)$ removes all volume integration terms in bilinear form $\mathcal{A}_{DG_F}(\cdot;\cdot)$, and DG formulation (4) reduces to:

Seek $(v_{Fh}, p_h) \subset \mathbf{V}(\mathcal{T}_h)$ *such that, for all* $(\omega_F, q) \subset \mathbf{V}(\mathcal{T}_h)$, *it holds:*

$$\begin{aligned}
& \int_{\mathcal{F}_h^{\Omega_F}} \Big[\frac{1}{c_F^2 \rho_F} p_h{}^- [\![q]\!]_t + \rho_F v_{Fh}{}^- [\![\omega_F]\!]_t\Big] d\mathrm{s} \\
& + \int_{\mathcal{F}_h^{I_F}} \Big[\{\!\{p_h\}\!\} [\![\omega_F]\!]_x + \{\!\{v_{Fh}\}\!\} [\![q]\!]_x + \alpha [\![v_{Fh}]\!]_x [\![\omega_F]\!]_x + \beta [\![p_h]\!]_x [\![q]\!]_x \Big] d\mathrm{s} \\
& + \int_{\mathcal{F}_h^{T_F}} \Big[\frac{1}{c_F^2 \rho_F} p_h q + \rho_F v_{Fh} \cdot \omega_F\Big] d\mathrm{s} - \frac{1}{2} \int_{\mathcal{F}_h^{0_F}} \Big[\frac{1}{c_F^2 \rho_F} p_h q + \rho_F v_{Fh} \cdot \omega_F\Big] d\mathrm{s} \\
& + \int_{\mathcal{F}_h^{D_F}} \Big[p n_{K_F}^x \cdot \omega_F + \alpha v_{Fh} \cdot \omega_F\Big] d\mathrm{s} = \\
& \frac{1}{2} \int_{\mathcal{F}_h^{0_F}} \Big[\frac{1}{c_F^2 \rho_F} p_h q + \rho_F v_{Fh} \cdot \omega_F\Big] d\mathrm{s} + \int_{\mathcal{F}_h^{D_F}} \Big[\alpha \mathrm{g}_{D_F} \cdot \omega_F - \mathrm{g}_{D_F} \cdot n_{K_F}^x q\Big] d\mathrm{s}.
\end{aligned} \tag{5}$$

Another advantage of Trefftz-DG formulation is that, compared to the classical DG formulation, it does not contain any differential operators.

Introducing bilinear $\mathcal{A}_{TDG_F}(\cdot\,;\cdot)$ and linear $\ell_{TDG_F}(\cdot)$ operators, (5) can be rewritten as follows:

Seek $(v_{Fh}, p_h) \subset \mathbf{V}(\mathcal{T}_h)$ *such that, for all* $(\omega_F, q) \subset \mathbf{V}(\mathcal{T}_h)$, *it holds*

$$\mathcal{A}_{TDG_F}((v_{Fh}, p_h); (\omega_F, q)) = \ell_{TDG_F}(\omega_F, q). \tag{6}$$

Once we have determined the discrete space $\mathbf{V}(\mathcal{T}_h)$, variational problem (6) can be solved as a global algebraic linear system [19, 23].

2.1.4 Well-posedness of Trefftz-DG formulation

In order to prove well-posedness of the Trefftz-DG method for AS, we need to prove the coercivity and continuity properties for (6) in a mesh-dependent norm.

The analysis is carried out inside the framework developed in [23] for the time-dependent Maxwell problem. For more details concerning the estimations, see Appendix A.1.

The mesh-dependent norm $|||\cdot|||_{TDG_F}$ in Trefftz space $\mathbf{T}_F(\mathcal{T}_h)$ can be defined as the coercive part of $\mathcal{A}_{TDG_F}((\omega_F, q); (\omega_F, q))$, written in terms of mesh-dependent L^2 norms:

$$\begin{aligned}
|||(\omega_F, q)|||^2_{TDG_F} \equiv & \frac{1}{2}\left\|\left(\frac{1}{c_F^2\rho_F}\right)^{1/2}[\![q]\!]_t\right\|^2_{L^2(\mathcal{F}_h^{\Omega_F})} + \frac{1}{2}\left\|\rho_F^{1/2}[\![\omega_F]\!]_t\right\|^2_{L^2(\mathcal{F}_h^{\Omega_F})} \\
& + \left\|\alpha^{1/2}[\![\omega_F]\!]_x\right\|^2_{L^2(\mathcal{F}_h^{I_F})} + \left\|\beta^{1/2}[\![q]\!]_x\right\|^2_{L^2(\mathcal{F}_h^{I_F})} \\
& + \frac{1}{2}\left\|\left(\frac{1}{c_F^2\rho_F}\right)^{1/2} q\right\|^2_{L^2(\mathcal{F}_h^{T_F})} + \frac{1}{2}\left\|\rho_F^{1/2}\omega_F\right\|^2_{L^2(\mathcal{F}_h^{T_F})} \\
& + \left\|\alpha^{1/2}\omega_F\right\|^2_{L^2(\mathcal{F}_h^{D_F})}.
\end{aligned}$$

Media parameters enter the $|||\cdot|||_{TDG_F}$ norm only through their traces on Ω-faces, where they are continuous. Thus, for all (ω_F, q) in $\mathbf{T}_F(\mathcal{T}_h)$ we obtain a coercivity property for $\mathcal{A}_{TDG_F}(\cdot,\cdot)$:

$$\mathcal{A}_{TDG_F}((\omega_F, q); (\omega_F, q)) = |||(\omega_F, q)|||^2_{TDG_F},\ \forall (\omega_F, q) \in \mathbf{T}_F(\mathcal{T}_h).$$

We also consider one "add-on" norm $|||(\omega_F, q)|||_{TDG^*_F}$ in $\mathbf{T}_F(\mathcal{T}_h)$. This norm has been computed, in order to use a weighted Cauchy-Schwarz inequality, to obtain continuity estimates for $\mathcal{A}_{TDG_F}(\cdot,\cdot)$:

$$\begin{aligned}
|||(\omega_F, q)|||^2_{TDG^*_F} \equiv & |||(\omega_F, q)|||^2_{TDG_F} + \|\alpha^{-1/2}\omega_F\|^2_{L^2(\mathcal{F}_h^{D_F})} \\
& + \|\rho_F^{1/2}\omega_F^-\|^2_{L^2(\mathcal{F}_h^{\Omega_F})} + \|\left(\frac{1}{c_F^2\rho_F}\right)^{1/2} q^-\|^2_{L^2(\mathcal{F}_h^{\Omega_F})} \\
& + \|\beta^{-1/2}\{\!\{\omega_F\}\!\}\|^2_{L^2(\mathcal{F}_h^{I_F})} + \|\alpha^{-1/2}\{\!\{q\}\!\}\|^2_{L^2(\mathcal{F}_h^{I_F})}.
\end{aligned}$$

Thus:

$$|\mathcal{A}_{TDG_F}((v_F, p); (\omega_F, q))| \le 2\,|||(v_F, p)|||_{TDG^*_F}|||(\omega_F, q)|||_{TDG_F},$$

$$|\ell_{TDG_F}(\omega_F, q)| \le \sqrt{2}\left[\|\rho_F^{1/2}v_{F0}\|^2_{L^2(\mathcal{F}_h^{0_F})} + \|\left(\frac{1}{c_F^2\rho_F}\right)^{1/2}p_0\|^2_{L^2(\mathcal{F}_h^{0_F})}\right]^{1/2}, \quad (\mathrm{g}_{D_F} \equiv 0).$$

The above inequalities confirm that variational problem (6) admits a unique solution $(v_{Fh}, p_h) \in \mathbf{V}(\mathcal{T}_h)$. Moreover, the following estimate holds true:

$$|||(v_F - v_{Fh}, p - p_h)|||_{TDG_F} \leq 3 \inf_{(\omega_F, q) \in \mathbf{V}(\mathcal{T}_h)} |||(v_F - \omega_F, p - q)|||_{TDG_F^*}.$$

2.2 Application to elastodynamics

As in the acoustic case, we consider first order ES and develop a discrete Trefftz-DG formulation. The analysis of well-posedness of final Trefftz-DG formulation is given at the end of this Section (here and further the subscript S corresponds to "Solid" - elastic media indicator).

2.3 Elastodynamic system

The Elastodynamic system is based on three fundamental laws of continuum mechanics: movement equations, constitutive equations (Hook's law), and geometric equations (infinitesimal strain tensor definition) [25].

As in the acoustic case, we introduce a global space-time domain $Q_S \equiv \Omega_S \times I$, which contains a bounded Lipschitz space domain $\Omega_S \subset R^n$ and a time interval $I \equiv (0, T)$.

The elastic modulus $\lambda \equiv \lambda(x)$, $\mu \equiv \mu(x)$ and solid density $\rho_S \equiv \rho_S(x)$ are solid parameters, piecewise constant and positive.

We consider first order ES in terms of velocity $v_S \equiv v_S(x,t)$ and stress $\underline{\underline{\sigma}} \equiv \underline{\underline{\sigma}}(x,t)$ fields:

$$\begin{cases} \dfrac{\partial \underline{\underline{\sigma}}}{\partial t} - \underline{\underline{C}}\,\underline{\underline{\varepsilon}}(v_S) = 0 \text{ in } Q_S, \\ \rho_S \dfrac{\partial v_S}{\partial t} - \mathrm{div}\underline{\underline{\sigma}} = 0 \text{ in } Q_S, \\ v_S(\cdot, 0) = v_{S0},\ \underline{\underline{\sigma}}(\cdot, 0) = \underline{\underline{\sigma}}_0 \text{ in } \Omega_S, \\ \underline{\underline{\sigma}} = \mathrm{g}_{D_S} \text{ in } \partial\Omega_S \times I, \end{cases}$$

where $\underline{\underline{C}}$ is the elastic coefficient tensor (symmetrical and positive), $\underline{\underline{\varepsilon}}(v_S) = \dfrac{1}{2}(\nabla v_S + \nabla v_S^T)$ is the infinitesimal strain tensor. The boundary conditions $\mathrm{g}_{D_S} \equiv \mathrm{g}_{D_S}(x,t)$, the velocity v_{s0} and the stress $\underline{\underline{\sigma}}_0$ are the initial data (further, the Dirichlet conditions will be imposed on $\partial\Omega_S$).

By symmetry and positivity of tensor $\underline{\underline{C}}$, the application $\underline{\underline{\varepsilon}} \longmapsto \underline{\underline{C}}\,\underline{\underline{\varepsilon}}$ is an isomorphism in the symmetrical tensor space [25]. Thus, we may consider the corresponding inverse application $\underline{\underline{A}}$, verifying the same properties of symmetry and positivity:

$$\begin{cases} \underline{\underline{A}} \dfrac{\partial \underline{\underline{\sigma}}}{\partial t} - \underline{\underline{\varepsilon}}(v_S) = 0 \text{ in } Q_S, \\ \rho_S \dfrac{\partial v_S}{\partial t} - \mathrm{div}\underline{\underline{\sigma}} = 0 \text{ in } Q_S, \\ v_S(\cdot, 0) = v_{S0},\ \underline{\underline{\sigma}}(\cdot, 0) = \underline{\underline{\sigma}}_0 \text{ in } \Omega_S, \\ \underline{\underline{\sigma}}_S = \mathrm{g}_{D_S} \text{ in } \partial\Omega_S \times I. \end{cases} \tag{7}$$

2.3.1 Space-time DG formulation

Formulations, similar to the acoustic case, can be obtained for elastodynamic problem. We chose Lipschitz sub-domain $K_S \subset Q_S$ such that λ, μ and ρ_S are constant in K_S. We chose $n_{K_S} = (n_{K_S}^x, n_{K_S}^t)$ is the outward pointing unit normal vector on ∂K_S and v_S, $\underline{\underline{\sigma}} \in H^1(K_S)$.

Multiplying both equations of (7) by the test functions txi, $\omega_S \in H^1(K_S)$ respectively, and integrating by parts in space and time, we obtain:

$$\begin{aligned} &-\int_{K_S}\Big[\underline{\underline{\sigma}} : (\underline{\underline{A}}\frac{\partial \underline{\underline{\xi}}}{\partial t} - \underline{\underline{\varepsilon}}(\omega_S)) + v_S \cdot (\rho_S \frac{\partial \omega_S}{\partial t} - \mathrm{div}\underline{\underline{\xi}})\Big] d\mathrm{v} \\ &+\int_{\partial K_S}\Big[\underline{\underline{A}}\,\underline{\underline{\sigma}} : \underline{\underline{\xi}} n^t_{K_S} - v_S \cdot n^x_{K_S}\underline{\underline{\xi}} + \rho_S v_S n^t_{K_S}\cdot\omega_S - \underline{\underline{\sigma}} n^x_{K_S}\cdot\omega_S\Big] d\mathrm{s} = 0. \end{aligned} \tag{8}$$

We introduce a non-overlapping mesh $\mathcal{T}_h$ on Q_S, which elements are right prisms, with vertical sides parallel to time axis. All solid parameters inside the elements K_S are supposed to be constant, so that all discontinuities lie on the inter-element boundaries.

Mesh skeleton $\mathcal{F}_h = \cup_{K_S\in\mathcal{T}_h}\partial K_S$ can be decomposed into families of element faces as follows:

$$\begin{aligned} \mathcal{F}_h^{\Omega_S} &- \text{ internal } \Omega\text{-faces } (t \text{ - fixed}),\\ \mathcal{F}_h^{I_S} &- \text{ internal } I\text{-faces } (x \text{ - fixed}),\\ \mathcal{F}_h^{0_S} &- \text{ external initial time faces } (\Omega_S\times\{0\}),\\ \mathcal{F}_h^{T_S} &- \text{ external final time faces } (\Omega_S\times\{T\}),\\ \mathcal{F}_h^{D_S} &- \text{ external Dirichlet boundary faces } (\partial\Omega_S\times[0,T]). \end{aligned}$$

The space-time DG formulation of the IBVP consists in searching $(v_{Sh}, \underline{\underline{\sigma}}_h) \subset \mathbf{V}(\mathcal{T}_h) \subset H^1(\mathcal{T}_h)^2$ such that, for all $K_S \in \mathcal{T}_h$ and for all $(\omega_S, \underline{\underline{\xi}}) \subset \mathbf{V}(\mathcal{T}_h)$ the following identity holds true:

$$\begin{aligned} &-\int_{K_S}\Big[\underline{\underline{\sigma}}_h : (\underline{\underline{A}}\frac{\partial \underline{\underline{\xi}}}{\partial t} - \underline{\underline{\varepsilon}}(\omega_S)) + v_{Sh} \cdot (\rho_S \frac{\partial \omega_S}{\partial t} - \mathrm{div}\underline{\underline{\xi}})\Big] d\mathrm{v} \\ &+\int_{\partial K_S}\Big[\underline{\underline{A}}\,\underline{\underline{\hat{\sigma}}}_h : \underline{\underline{\xi}} n^t_{K_S} - \hat{v_{Sh}} \cdot n^x_{K_S}\underline{\underline{\xi}} + \rho_S \hat{v_{Sh}} n^t_{K_S}\cdot\omega_S - \underline{\underline{\hat{\sigma}}}_h n^x_{K_S}\cdot\omega_S\Big] d\mathrm{s} = 0. \end{aligned} \tag{9}$$

The numerical fluxes $\hat{v_{Sh}}$, $\underline{\underline{\hat{\sigma}}}_h$ are defined on the mesh skeleton $\mathcal{F}_h$ as follows:

$$\begin{aligned} \begin{pmatrix}\hat{v_{Sh}}\\ \underline{\underline{\hat{\sigma}}}_h\end{pmatrix} &\equiv \begin{pmatrix}\{\!\{v_{Sh}\}\!\} - \delta[\![\underline{\underline{\sigma}}_h]\!]_x\\ \{\!\{\underline{\underline{\sigma}}_h\}\!\} - \gamma[\![v_{Sh}]\!]_x\end{pmatrix} && \text{on } \mathcal{F}_h^{I_S},\\ \begin{pmatrix}\hat{v_{Sh}}\cdot n^x_{K_S}\\ \underline{\underline{\hat{\sigma}}}_h n^x_{K_S}\end{pmatrix} &\equiv \begin{pmatrix}v_{Sh}\cdot n^x_{K_S} - \delta(\underline{\underline{\sigma}}_h - \mathrm{g}_{D_S})n^x_{K_S}\\ \mathrm{g}_{D_S} n^x_{K_S}\end{pmatrix} && \text{on } \mathcal{F}_h^{D_S},\\ \begin{pmatrix}\hat{v_{Sh}}\\ \underline{\underline{\hat{\sigma}}}_h\end{pmatrix} &\equiv \begin{pmatrix}v_{Sh}^-\\ \underline{\underline{\sigma}}_h^-\end{pmatrix} && \text{on } \mathcal{F}_h^{\Omega_S},\\ \begin{pmatrix}\hat{v_{Sh}}\\ \underline{\underline{\hat{\sigma}}}_h\end{pmatrix} &\equiv \begin{pmatrix}v_{Sh}\\ \underline{\underline{\sigma}}_h\end{pmatrix} && \text{on } \mathcal{F}_h^{T_S},\\ \begin{pmatrix}\hat{v_{Sh}}\\ \underline{\underline{\hat{\sigma}}}_h\end{pmatrix} &\equiv \begin{pmatrix}v_{S0}\\ \underline{\underline{\sigma}}_0\end{pmatrix} && \text{on } \mathcal{F}_h^{0_S}. \end{aligned}$$

Here $\delta \in L^\infty(\mathcal{F}_h^{I_S}\cup\mathcal{F}_h^{D_S})$ and $\gamma \in L^\infty(\mathcal{F}_h^{I_S})$ are positive penalty parameters. One can notice some differences between the flux definition in the acoustic and elastic cases for I-faces and Dirichlet faces. This choice is recommended in order to improve the numerical stability of the scheme (see [2, 7, 8, 10] to learn more about possible choices of penalty terms).

Summing over all elements $K_S \in \mathcal{T}_h$, we obtain a DG formulation for (7).
Seek $(v_{Sh}, \underline{\underline{\sigma}}_h) \subset \mathbf{V}(\mathcal{T}_h)$ *such that, for all* $(\omega_S, \underline{\underline{\xi}}) \subset \mathbf{V}(\mathcal{T}_h)$, *it holds:*

$$
\begin{aligned}
&\sum_{K_S \in \mathcal{T}_h} -\int_{K_S} \Big[\underline{\underline{\sigma}}_h : (\underline{\underline{A}}\frac{\partial \underline{\underline{\xi}}}{\partial t} - \underline{\underline{\varepsilon}}(\omega_S)) + v_{Sh}(\rho_S \frac{\partial \omega_S}{\partial t} - \mathrm{div}\underline{\underline{\xi}})\Big] d\mathrm{v} \\
&\quad + \int_{\mathcal{F}_h^{\Omega_S}} \Big[\underline{\underline{A}}\,\underline{\underline{\sigma}}_h{}^{-} : [\![\underline{\underline{\xi}}]\!]_t + \rho_S v_{Sh}{}^{-}[\![\omega_S]\!]_t\Big] d\mathrm{s} \\
&\quad - \int_{\mathcal{F}_h^{I_S}} \Big[\{\underline{\underline{\sigma}}_h\}[\![\omega_S]\!]_x + \{v_{Sh}\}[\![\underline{\underline{\xi}}]\!]_x - \gamma[\![v_{Sh}]\!]_x[\![\omega_S]\!]_x - \delta[\![\underline{\underline{\sigma}}_h]\!]_x[\![\underline{\underline{\xi}}]\!]_x\Big] d\mathrm{s} \\
&\quad + \int_{\mathcal{F}_h^{T_S}} \Big[\underline{\underline{A}}\,\underline{\underline{\sigma}}_h : \underline{\underline{\xi}} + \rho_S v_{Sh}\cdot\omega_S\Big] d\mathrm{s} - \frac{1}{2}\int_{\mathcal{F}_h^{0_S}} \Big[\underline{\underline{A}}\,\underline{\underline{\sigma}}_h : \underline{\underline{\xi}} + \rho_S v_{Sh}\cdot\omega_S\Big] d\mathrm{s} \\
&\quad - \int_{\mathcal{F}_h^{D_S}} \Big[v_{Sh}\cdot n^x_{K_S}\underline{\underline{\xi}} - \delta\underline{\underline{\sigma}}_h : \underline{\underline{\xi}}\Big] d\mathrm{s} = \\
&\qquad \frac{1}{2}\int_{\mathcal{F}_h^{0_S}} \Big[\underline{\underline{A}}\,\underline{\underline{\sigma}}_h : \underline{\underline{\xi}} + \rho_S v_{Sh}\cdot\omega_S\Big] d\mathrm{s} + \int_{\mathcal{F}_h^{D_S}} \Big[\mathrm{g}_{D_S} n^x_{K_S}\cdot\omega_S + \delta \mathrm{g}_{D_S} : \underline{\underline{\xi}})\Big] d\mathrm{s}.
\end{aligned}
\tag{10}
$$

2.3.2 Trefftz space. Trefftz-DG formulation

We define the Trefftz space in elastic media:

$$
\mathbf{T}_S(\mathcal{T}_h) \equiv \Big\{(\omega_S, \underline{\underline{\xi}}) \subset H^1(\mathcal{T}_h)^2 \text{ s. t. } \rho_S \frac{\partial \omega_S}{\partial t} - \mathrm{div}\underline{\underline{\xi}} = \underline{\underline{A}}\frac{\partial \underline{\underline{\xi}}}{\partial t} - \underline{\underline{\varepsilon}}(\omega_S) = 0 \text{ in all } K_S \in \mathcal{T}_h\Big\}.
$$

By this choice of discrete space, DG formulation (10) reduces to:
Seek $(v_{Sh}, \underline{\underline{\sigma}}_h) \subset \mathbf{V}(\mathcal{T}_h)$ *such that, for all* $(\omega_S, \underline{\underline{\xi}}) \subset \mathbf{V}(\mathcal{T}_h)$, *it holds:*

$$
\begin{aligned}
&\int_{\mathcal{F}_h^{\Omega_S}} \Big[\underline{\underline{A}}\,\underline{\underline{\sigma}}_h{}^{-} : [\![\underline{\underline{\xi}}]\!]_t + \rho_S v_{Sh}{}^{-}[\![\omega_S]\!]_t\Big] d\mathrm{s} \\
&- \int_{\mathcal{F}_h^{I_S}} \Big[\{\underline{\underline{\sigma}}_h\}[\![\omega_S]\!]_x + \{v_{Sh}\}[\![\underline{\underline{\xi}}]\!]_x - \gamma[\![v_{Sh}]\!]_x[\![\omega_S]\!]_x - \delta[\![\underline{\underline{\sigma}}_h]\!]_x[\![\underline{\underline{\xi}}]\!]_x\Big] d\mathrm{s} \\
&+ \int_{\mathcal{F}_h^{T_S}} \Big[\underline{\underline{A}}\,\underline{\underline{\sigma}}_h : \underline{\underline{\xi}} + \rho_S v_{Sh}\cdot\omega_S\Big] d\mathrm{s} - \frac{1}{2}\int_{\mathcal{F}_h^{0_S}} \Big[\underline{\underline{A}}\,\underline{\underline{\sigma}}_h : \underline{\underline{\xi}} + \rho_S v_{Sh}\cdot\omega_S\Big] d\mathrm{s} \\
&- \int_{\mathcal{F}_h^{D_S}} \Big[v_{Sh}\cdot n^x_{K_S}\underline{\underline{\xi}} - \delta\underline{\underline{\sigma}}_h : \underline{\underline{\xi}}\Big] d\mathrm{s} = \\
&\quad \frac{1}{2}\int_{\mathcal{F}_h^{0_S}} \Big[\underline{\underline{A}}\,\underline{\underline{\sigma}}_h : \underline{\underline{\xi}} + \rho_S v_{Sh}\cdot\omega_S\Big] d\mathrm{s} + \int_{\mathcal{F}_h^{D_S}} \Big[\mathrm{g}_{D_S} n^x_{K_S}\cdot\omega_S + \delta \mathrm{g}_{D_S} : \underline{\underline{\xi}})\Big] d\mathrm{s},
\end{aligned}
$$

or, by introducing bilinear $\mathcal{A}_{TDG_F}(\cdot\,;\cdot)$ and linear $\ell_{TDG_F}(\cdot)$ operators:
Seek $(v_{Sh}, \underline{\underline{\sigma}}_h) \subset \mathbf{V}(\mathcal{T}_h)$ *such that, for all* $(\omega_S, \underline{\underline{\xi}}) \subset \mathbf{V}(\mathcal{T}_h)$, *it holds:*

$$
\mathcal{A}_{TDG_S}((v_{Sh}, \underline{\underline{\sigma}}_h); (\omega_S, \underline{\underline{\xi}})) = \ell_{TDG_S}(\omega_s, \underline{\underline{\xi}}). \tag{11}
$$

2.3.3 Well-posedness of Trefftz-DG formulation

By analogy with the acoustic model, we obtain in this section the coercivity and continuity estimates proving well-posedness of the obtained Trefftz-DG method for ES in mesh-dependent norms (see Appendix A.2 for more details).

We introduce two mesh-dependent norms in $\mathbf{T}_S(\mathcal{T}_h)$:

$$\begin{aligned}
|||(\omega_S,\underline{\underline{\xi}})|||^2_{TDG_S} \equiv & \frac{1}{2}\left\|(\underline{\underline{A}})^{1/2}[\![\underline{\underline{\xi}}]\!]_t\right\|^2_{L^2(\mathcal{F}_h^{\Omega_S})} + \frac{1}{2}\left\|\rho_S^{1/2}[\![\omega_S]\!]_t\right\|^2_{L^2(\mathcal{F}_h^{\Omega_S})} \\
& + \left\|\gamma^{1/2}[\![\omega_S]\!]_x\right\|^2_{L^2(\mathcal{F}_h^{I_S})} + \left\|\delta^{1/2}[\![\underline{\underline{\xi}}]\!]_x\right\|^2_{L^2(\mathcal{F}_h^{I_S})} \\
& + \frac{1}{2}\left\|(\underline{\underline{A}})^{1/2}\underline{\underline{\xi}}\right\|^2_{L^2(\mathcal{F}_h^{T_S})} + \frac{1}{2}\left\|\rho_S^{1/2}\omega_S\right\|^2_{L^2(\mathcal{F}_h^{T_S})} \\
& + \left\|\delta^{1/2}\underline{\underline{\xi}}\right\|^2_{L^2(\mathcal{F}_h^{D_S})},
\end{aligned}$$

$$\begin{aligned}
|||(\omega_S,\underline{\underline{\xi}})|||^2_{TDG_S^*} \equiv & |||(\omega_S,\underline{\underline{\xi}})|||^2_{TDG_S} \\
& + \|\rho_S^{1/2}\omega_S^-\|^2_{L^2(\mathcal{F}_h^{\Omega_S})} + \|(\underline{\underline{A}})^{1/2}\underline{\underline{\xi}}^-\|^2_{L^2(\mathcal{F}_h^{\Omega_S})} \\
& + \|\delta^{-1/2}\{\omega_S\}\|^2_{L^2(\mathcal{F}_h^{I_S})} + \|\gamma^{-1/2}\{\underline{\underline{\xi}}\}\|^2_{L^2(\mathcal{F}_h^{I_S})} \\
& + \|\delta^{-1/2}\underline{\underline{\xi}}\|^2_{L^2(\mathcal{F}_h^{D_S})}.
\end{aligned}$$

Thus, for the bilinear $\mathcal{A}_{TDG_S}(\cdot,\cdot)$ and linear $\ell_{TDG_S}(\cdot)$ forms we obtain the following coercivity

$$\mathcal{A}_{TDG_S}((\omega_S,\underline{\underline{\xi}});(\omega_S,\underline{\underline{\xi}})) = |||(\omega_S,\underline{\underline{\xi}})|||^2_{TDG_S},\ \forall(\omega_S,\underline{\underline{\xi}}) \in \mathbf{T}_S(\mathcal{T}_h),$$

and continuity properties

$$\begin{aligned}
& |\mathcal{A}_{TDG_S}((v_S,\underline{\underline{\sigma}});(\omega_S,\underline{\underline{\xi}}))| \le 2\,|||(v_S,\underline{\underline{\sigma}})|||_{TDG_S^*}|||(\omega_S,\underline{\underline{\xi}})|||_{TDG_S}, \\
& |\ell_{TDG_S}(\omega_S,\underline{\underline{\xi}})| \le \sqrt{2}\left[\|\rho_S^{1/2}v_{S0}\|^2_{L^2(\mathcal{F}_h^{0_S})} + \|\underline{\underline{A}}^{1/2}\underline{\underline{\sigma}}_0\|^2_{L^2(\mathcal{F}_h^{0_S})}\right]^{1/2}, \quad (g_{D_S} \equiv 0).
\end{aligned}$$

with respect to the chosen norms.

The above estimates confirm well-posedness of the Trefftz-DG problem for ES, moreover:

$$|||(v_S - v_{Sh},\underline{\underline{\sigma}} - \underline{\underline{\sigma}}_h)|||_{TDG_S} \le 3 \inf_{(\omega_S,\underline{\underline{\xi}})\in\mathbf{V}(\mathcal{T}_h)} |||(v_S - \omega_S,\underline{\underline{\sigma}} - \underline{\underline{\xi}})|||_{TDG_S^*}.$$

2.4 Application to elasto-acoustics

It is well known that acoustic media can be considered as a limit case of elastic isotropic media, with shear modulus μ tending or equal to zero [1]. Thus, it might be possible to solve first the elastodynamic problem with variable coefficients, and then, to treat acoustic media as a particular region of heterogeneous elastic media with the shear modulus $\mu \equiv 0$ or very small.

From a practical point of view, solving ES requires computing six components of stress tensor in acoustic media instead of one necessary unknown - pressure. Mathematically, if the numerical code is based on discretization by H^1 finite elements , considering $\mu \equiv 0$ destroys the coercivity of H^1 norms, and the choice of a very small μ provides numerical artefacts, due to a slow S - waves appearance. An example of this phenomena has been observed by Bossy in [9].

Methods based on discontinuous finite element approximation are basically well-adapted to specific fluid-solid interaction problems. They require solving a transmission problem between

acoustic and elastodynamic systems in terms of velocity - pressure in fluid and velocity - stress in solid.

In this section we introduce EAS based on the numerical coupling of proper AS (1) and ES (7) by the transmission conditions. We will use the results and notations, introduced previously for the acoustic and elastic cases, to apply Trefftz-DG approximation to the coupled EAS, and to analyze well-posedness of the problem.

2.4.1 Transmission conditions. Coupled elasto-acoustic system.

The choice of the transmission conditions $\Gamma_{FS} \equiv \partial\Omega_F \cap \partial\Omega_S$ requires the continuity of velocity and stress normal components at the interface. The shear stress must vanish at the interface, and velocities aligned to the interface remain unconstrained [12, 25]:

$$\begin{cases} v_F \cdot n_{\Gamma_{FS}} = v_S \cdot n_{\Gamma_{FS}} \text{ at } \Gamma_{FS}, \\ \underline{\underline{\sigma}} n_{\Gamma_{FS}} = -p n_{\Gamma_{FS}} \text{ at } \Gamma_{FS}, \end{cases} \tag{12}$$

where $n_{\Gamma_{FS}}$ is a unit normal vector to Γ_{FS}.

Multiplying (12) by test functions q and ω_S respectively, and integrating by parts in time and space, we obtain the following identities:

$$\begin{aligned} \int_{\Gamma_{FS}} (v_F \cdot n^x_\Omega) q d\mathrm{s} &= \int_{\Gamma_{FS}} (v_S \cdot n^x_\Omega) q d\mathrm{s}, \\ \int_{\Gamma_{FS}} (\underline{\underline{\sigma}} n^x_\Omega) \cdot \omega_S d\mathrm{s} &= -\int_{\Gamma_{FS}} (p n^x_\Omega) \cdot \omega_S d\mathrm{s}. \end{aligned} \tag{13}$$

We will apply (13) to the in-coming and out-going flux terms at Γ_{FS}, to couple previously obtained formulations for AS and ES.

The mesh $\mathcal{T}_h$ on $Q \equiv Q_F \cup Q_S$ is composed of the meshes previously defined on Q_F and Q_S, with the mesh skeleton $\mathcal{F}_h = \cup_{K\in\mathcal{T}_h} \partial K$ and its subsets:

$\mathcal{F}_h^{\Omega_F}$ – internal Ω-faces in fluid (t - fixed),
$\mathcal{F}_h^{I_F}$ – internal I-faces in fluid (x - fixed)
$\mathcal{F}_h^{0_F}$ – external initial time faces ($\Omega_F \times \{0\}$),
$\mathcal{F}_h^{T_F}$ – external final time faces ($\Omega_F \times \{T\}$),
$\mathcal{F}_h^{D_F}$ – external Dirichlet boundary faces ($\partial\Omega_F \times [0,T]$),
$\mathcal{F}_h^{\Omega_S}$ – internal Ω-faces in solid (t - fixed),
$\mathcal{F}_h^{I_S}$ – internal I-faces in solid (x - fixed),
$\mathcal{F}_h^{0_S}$ – external initial time faces ($\Omega_S \times \{0\}$),
$\mathcal{F}_h^{T_S}$ – external final time faces ($\Omega_S \times \{T\}$),
$\mathcal{F}_h^{D_S}$ – external Dirichlet boundary faces ($\partial\Omega_S \times [0,T]$),
$\mathcal{F}_h^{FS}$ – internal fluid-solid interface faces ($\Gamma_{FS} \times [0,T]$).

2.4.2 Space-time DG formulation

We look for a discrete solution $(v_{Fh}, p_h, v_{Sh}, \underline{\underline{\sigma}}_h)$ for $(v_F, p, v_s, \underline{\underline{\sigma}})$ in $\mathbf{V}(\mathcal{T}_h) \subset H^1(\mathcal{T}_h)^4$.

The space-time DG discretization of the coupled problem consists in finding $(v_{Fh}, p_h, v_{Sh}, \underline{\underline{\sigma}}_h) \subset \mathbf{V}(\mathcal{T}_h)$ such that, for all $K_F, K_S \in \mathcal{T}_h$ and for all $(\omega_F, q, \omega_S, \underline{\underline{\xi}}) \subset \mathbf{V}(\mathcal{T}_h)$ it holds true:

$$
\begin{aligned}
&-\int_{K_F} \Big[p_h(\frac{1}{c_F^2\rho_F}\frac{\partial q}{\partial t} + \mathrm{div}\omega_F) + v_{Fh}\cdot(\rho_F\frac{\partial \omega_F}{\partial t} + \nabla q)\Big]d\mathrm{v} \\
&+\int_{\partial K_F}\Big[\frac{1}{c_F^2\rho_F}\hat{p_h}n_{K_F}^t q + v_{\hat{F}h}\cdot n_{K_F}^x q + \rho_F v_{\hat{F}h} n_{K_F}^t\cdot\omega_F + \hat{p_h}n_{K_F}^x\cdot\omega_F\Big]d\mathrm{s} = \int_{K_F} fq d\mathrm{v}, \\
&-\int_{K_S}\Big[\underline{\underline{\sigma}}_h : (\underline{\underline{A}}\frac{\partial \underline{\underline{\xi}}}{\partial t} - \underline{\underline{\varepsilon}}(\omega_S)) + v_{Sh}\cdot(\rho_S\frac{\partial\omega_S}{\partial t} - \mathrm{div}\underline{\underline{\xi}})\Big]d\mathrm{v} \\
&+\int_{\partial K_S}\Big[\underline{\underline{A}}\,\hat{\underline{\underline{\sigma}}}_h : \underline{\underline{\xi}}n_{K_S}^t - v_{\hat{S}h}\cdot n_{K_S}^x\underline{\underline{\xi}} + \rho_S v_{\hat{S}h}n_{K_S}^t\cdot\omega_S - \hat{\underline{\underline{\sigma}}}_h n_{K_S}^x\cdot\omega_S\Big]d\mathrm{s} = 0.
\end{aligned}
$$

The numerical fluxes $v_{\hat{F}h}$, $\hat{p_h}$, $v_{\hat{S}h}$, $\hat{\underline{\underline{\sigma}}}_h$ are defined on the mesh skeleton $\mathcal{F}_h$ as follows:

$$
\begin{aligned}
\begin{pmatrix} v_{\hat{F}h} \\ \hat{p_h}\end{pmatrix} &\equiv \begin{pmatrix} \{\!\{v_{Fh}\}\!\} + \beta[\![p_h]\!]_x \\ \{\!\{p_h\}\!\} + \alpha[\![v_{Fh}]\!]_x\end{pmatrix} && \text{on } \mathcal{F}_h^{I_F}, \\
\begin{pmatrix} v_{\hat{S}h} \\ \hat{\underline{\underline{\sigma}}}_h\end{pmatrix} &\equiv \begin{pmatrix} \{\!\{v_{Sh}\}\!\} - \delta[\![\underline{\underline{\sigma}}_h]\!]_x \\ \{\!\{\underline{\underline{\sigma}}_h\}\!\} - \gamma[\![v_{Sh}]\!]_x\end{pmatrix} && \text{on } \mathcal{F}_h^{I_S}, \\
\begin{pmatrix} v_{\hat{F}h}\cdot n_{K_F}^x \\ \hat{p_h}n_{K_F}^x\end{pmatrix} &\equiv \begin{pmatrix} \mathrm{g}_{D_F}\cdot n_{K_F}^x \\ p_h n_{K_F}^x + \alpha(v_{Fh} - \mathrm{g}_{D_F})\cdot n_{K_F}^x\end{pmatrix} && \text{on } \mathcal{F}_h^{D_F}, \\
\begin{pmatrix} v_{\hat{S}h}\cdot n_{K_S}^x \\ \hat{\underline{\underline{\sigma}}}_h n_{K_S}^x\end{pmatrix} &\equiv \begin{pmatrix} v_{Sh}\cdot n_{K_S}^x - \delta(\underline{\underline{\sigma}}_h - \mathrm{g}_{D_S})n_{K_S}^x \\ \mathrm{g}_{D_S}n_{K_S}^x\end{pmatrix} && \text{on } \mathcal{F}_h^{D_S}, \\
\begin{pmatrix} v_{\hat{F}h} \\ \hat{p_h}\end{pmatrix} &\equiv \begin{pmatrix} v_{Fh}^- \\ p_h^-\end{pmatrix} && \text{on } \mathcal{F}_h^{\Omega_F}, \\
\begin{pmatrix} v_{\hat{S}h} \\ \hat{\underline{\underline{\sigma}}}_h\end{pmatrix} &\equiv \begin{pmatrix} v_{Sh}^- \\ \underline{\underline{\sigma}}_h^-\end{pmatrix} && \text{on } \mathcal{F}_h^{\Omega_S}, \\
\begin{pmatrix} v_{\hat{F}h} \\ \hat{p_h}\end{pmatrix} &\equiv \begin{pmatrix} v_{Fh} \\ p_h\end{pmatrix} && \text{on } \mathcal{F}_h^{T_F}, \\
\begin{pmatrix} v_{\hat{S}h} \\ \hat{\underline{\underline{\sigma}}}_h\end{pmatrix} &\equiv \begin{pmatrix} v_{Sh} \\ \underline{\underline{\sigma}}_h\end{pmatrix} && \text{on } \mathcal{F}_h^{T_S}, \\
\begin{pmatrix} v_{\hat{F}h} \\ \hat{p_h}\end{pmatrix} &\equiv \begin{pmatrix} v_{F0} \\ p_0\end{pmatrix} && \text{on } \mathcal{F}_h^{0_F}, \\
\begin{pmatrix} v_{\hat{S}h} \\ \hat{\underline{\underline{\sigma}}}_h\end{pmatrix} &\equiv \begin{pmatrix} v_{S0} \\ \underline{\underline{\sigma}}_0\end{pmatrix} && \text{on } \mathcal{F}_h^{0_S}, \\
\begin{pmatrix} v_{\hat{F}h}\cdot n_{K_F}^x \\ \hat{p_h}n_{K_F}^x \\ v_{\hat{S}h}\cdot n_{K_S}^x \\ \hat{\underline{\underline{\sigma}}}_h n_{K_S}^x\end{pmatrix} &\equiv \begin{pmatrix} v_{Sh}\cdot n_{K_F}^x \\ p_h n_{K_F}^x + \alpha(v_{Fh}\cdot n_{K_F}^x - v_{Sh}\cdot n_{K_F}^x) \\ v_{Sh}\cdot n_{K_S}^x - \delta(\underline{\underline{\sigma}}_h n_{K_S}^x - p_h n_{K_S}^x) \\ -p_h n_{K_S}^x\end{pmatrix} && \text{on } \mathcal{F}_h^{FS}.
\end{aligned}
$$

2.4.3 Trefftz-DG formulation

We define the Trefftz space in elasto-acoustic media:

$$\mathbf{T}(\mathcal{T}_h) \equiv \Big\{ (\omega_F, q, \omega_S, \underline{\underline{\xi}}) \subset H^1(\mathcal{T}_h)^4 \text{ s. t. } \rho_F \frac{\partial \omega_F}{\partial t} + \nabla q = \frac{1}{c_F^2 \rho_F} \frac{\partial q}{\partial t} + \mathrm{div}\omega_F = 0$$
$$\text{in all } K_F \in \mathcal{T}_h,\ \rho_S \frac{\partial \omega_S}{\partial t} - \mathrm{div}\underline{\underline{\xi}} = \frac{\partial \underline{\underline{A}}\,\underline{\underline{\xi}}}{\partial t} - \underline{\underline{\varepsilon}}(\omega_S) = 0 \text{ in all } K_S \in \mathcal{T}_h \Big\}.$$

Thus, Trefftz-DG formulation for EAS reads as:

Seek $(v_{Fh}, p_h, v_{Sh}, \underline{\underline{\sigma}}_h) \subset \mathbf{V}(\mathcal{T}_h)$ *such that, for all* $(\omega_F, q, \omega_S, \underline{\underline{\xi}}) \subset \mathbf{V}(\mathcal{T}_h)$, *it holds:*

$$\int_{\mathcal{F}_h^{\Omega_F}} \Big[\frac{1}{c_F^2 \rho_F} p_h{}^{-} [\![q]\!]_t + \rho_F v_{Fh}{}^{-} [\![\omega_F]\!]_t \Big] d\mathrm{s}$$
$$+ \int_{\mathcal{F}_h^{I_F}} \Big[\{\!\{p_h\}\!\} [\![\omega_F]\!]_x + \{\!\{v_{Fh}\}\!\} [\![q]\!]_x + \alpha [\![v_{Fh}]\!]_x [\![\omega_F]\!]_x + \beta [\![p_h]\!]_x [\![q]\!]_x \Big] d\mathrm{s}$$
$$+ \int_{\mathcal{F}_h^{T_F}} \Big[\frac{1}{c_F^2 \rho_F} p_h n_{K_F}^t q + \rho_F v_{Fh} n_{K_F}^t \cdot \omega_F \Big] d\mathrm{s} - \frac{1}{2} \int_{\mathcal{F}_h^{0_F}} \Big[\frac{1}{c_F^2 \rho_F} p_h n_{K_F}^t q + \rho_F v_{Fh} n_{K_F}^t \cdot \omega_F \Big] d\mathrm{s}$$
$$+ \int_{\mathcal{F}_h^{D_F}} \Big[p n_{K_F}^x \cdot \omega_F + \alpha v_{Fh} \cdot \omega_F \Big] d\mathrm{s}$$
$$+ \int_{\mathcal{F}_h^{F_S}} \Big[p_h n_{K_F}^x \cdot \omega_F + \alpha (v_{Fh} \cdot n_{K_F}^x - v_{Sh} \cdot n_{K_F}^x) \cdot \omega_F + v_{Sh} \cdot n_{K_F}^x q) \Big] d\mathrm{s} =$$
$$\frac{1}{2} \int_{\mathcal{F}_h^{0_F}} \Big[\frac{1}{c_F^2 \rho_F} p_h q + \rho_F v_{Fh} \cdot \omega_F \Big] d\mathrm{s} + \int_{\mathcal{F}_h^{D_F}} \Big[\alpha \mathrm{g}_{D_F} \cdot \omega_F - \mathrm{g}_{D_F} \cdot n_{K_F}^x q \Big] d\mathrm{s},$$

$$\int_{\mathcal{F}_h^{\Omega_S}} \Big[\underline{\underline{A}}\,\underline{\underline{\sigma}}_h{}^{-} : [\![\underline{\underline{\xi}}]\!]_t + \rho_S v_{Sh}{}^{-} [\![\omega_S]\!]_t \Big] d\mathrm{s}$$
$$- \int_{\mathcal{F}_h^{I_S}} \Big[\{\!\{\underline{\underline{\sigma}}_h\}\!\} [\![\omega_S]\!]_x + \{\!\{v_{Sh}\}\!\} [\![\underline{\underline{\xi}}]\!]_x - \gamma [\![v_{Sh}]\!]_x [\![\omega_S]\!]_x - \delta [\![\underline{\underline{\sigma}}_h]\!]_x [\![\underline{\underline{\xi}}]\!]_x \Big] d\mathrm{s}$$
$$+ \int_{\mathcal{F}_h^{T_S}} \Big[\underline{\underline{A}}\,\underline{\underline{\sigma}}_h : \underline{\underline{\xi}} + \rho_S v_{Sh} \cdot \omega_S \Big] d\mathrm{s} - \frac{1}{2} \int_{\mathcal{F}_h^{0_S}} \Big[\underline{\underline{A}}\,\underline{\underline{\sigma}}_h : \underline{\underline{\xi}} + \rho_S v_{Sh} \cdot \omega_S \Big] d\mathrm{s}$$
$$- \int_{\mathcal{F}_h^{D_S}} \Big[v_{Sh} \cdot n_{K_S}^x \underline{\underline{\xi}} - \delta \underline{\underline{\sigma}}_h : \underline{\underline{\xi}} \Big] d\mathrm{s}$$
$$- \int_{\mathcal{F}_h^{F_S}} \Big[v_{Sh} \cdot n_{K_S}^x \underline{\underline{\xi}} - \delta (\underline{\underline{\sigma}}_h n_{K_S}^x - p_h n_{K_S}^x) \underline{\underline{\xi}} - p n_{K_S}^x \cdot \omega_S \Big] d\mathrm{s} =$$
$$\frac{1}{2} \int_{\mathcal{F}_h^{0_S}} \Big[\underline{\underline{A}}\,\underline{\underline{\sigma}}_h : \underline{\underline{\xi}} + \rho_S v_{Sh} \cdot \omega_S \Big] d\mathrm{s} + \int_{\mathcal{F}_h^{D_S}} \Big[\mathrm{g}_{D_S} n_{K_S}^x \cdot \omega_S + \delta \mathrm{g}_{D_S} : \underline{\underline{\xi}}) \Big] d\mathrm{s},$$

which can be rewritten, using bilinear $\mathcal{A}_{TDG}(\cdot\,;\cdot)$ and linear $\ell_{TDG}(\cdot)$ operators as follows:

Seek $(v_{Fh}, p_h, v_{Sh}, \underline{\underline{\sigma}}_h) \subset \mathbf{V}(\mathcal{T}_h)$ *such that, for all* $(\omega_F, q, \omega_S, \underline{\underline{\xi}}) \subset \mathbf{V}(\mathcal{T}_h)$, *it holds true:*

$$\mathcal{A}_{TDG}((v_{Fh}, p_h, v_{Sh}, \underline{\underline{\sigma}}_h); (\omega_F, q, \omega_S, \underline{\underline{\xi}})) = \ell_{TDG}(\omega_F, q, \omega_S, \underline{\underline{\xi}}). \tag{14}$$

2.4.4 Well-posedness of Trefftz-DG formulation

We will take into account the results obtained previously for acoustic and elastic problems in order to obtain coercivity and continuity estimations of $\mathcal{A}_{TDG}(\cdot\,;\cdot)$ and $\ell_{TDG}(\cdot)$ in the coupled

case (see Appendix A.3 for more details).

We introduce two mesh-dependent norms in $\mathbf{T}(\mathcal{T}_h)$:

$$|||(\omega_F, q, \omega_S, \underline{\underline{\xi}}))|||^2_{TDG} \equiv |||(\omega_F, q)|||^2_{TDG_F} + |||(\omega_S, \underline{\underline{\xi}})|||^2_{TDG_S} + 2\|\delta^{1/2}\underline{\underline{\xi}}\|^2_{L^2(\mathcal{F}_h^{FS})},$$

$$|||(\omega_F, q, \omega_S, \underline{\underline{\xi}})|||^2_{TDG^*} \equiv |||(\omega_F, q)|||^2_{TDG^*_F} + |||(\omega_S, \underline{\underline{\xi}})|||^2_{TDG^*_S} + \frac{1}{2}\|\alpha^{-1/2}\underline{\underline{\xi}}\|^2_{L^2(\mathcal{F}_h^{FS})}.$$

With respect to the chosen norms, for the bilinear $\mathcal{A}_{TDG}(\cdot,\cdot)$ and linear $\ell_{TDG}(\cdot)$ forms we obtain the coercivity

$$\mathcal{A}_{TDG}((\omega_F, q, \omega_S, \underline{\underline{\xi}}); (\omega_F, q, \omega_S, \underline{\underline{\xi}})) = |||(\omega_F, q, \omega_S, \underline{\underline{\xi}})|||^2_{TDG},$$

and continuity estimations

$$|\mathcal{A}_{TDG}((v_F, p, v_S, \underline{\underline{\sigma}}); (\omega_F, q, \omega_S, \underline{\underline{\xi}}))| \leq 2\,|||(v_F, p, v_S, \underline{\underline{\sigma}})|||_{TDG^*}\,|||(\omega_F, q\omega_S, \underline{\underline{\xi}})|||_{TDG},$$

$$|\ell_{TDG}(\omega_F, q, \omega_S, \underline{\underline{\xi}})| \leq \sqrt{2}\left[\|\rho_F^{1/2} v_{F0}\|^2_{L^2(\mathcal{F}_h^{0F})} + \|(\frac{1}{c_F^2\rho_F})^{1/2} p_0\|^2_{L^2(\mathcal{F}_h^{0F})}\right.$$
$$\left. +\ \|\rho_S^{1/2} v_{S0}\|^2_{L^2(\mathcal{F}_h^{0S})} + \|\underline{\underline{A}}^{1/2}\underline{\underline{\sigma}}_0\|^2_{L^2(\mathcal{F}_h^{0S})}\right]^{1/2}, \quad (\mathrm{g}_{D_F} = \mathrm{g}_{D_S} \equiv 0).$$

By Céa lemma, the variational problem (14) admits a unique solution $(v_{Fh}, p_h, v_{Sh}, \underline{\underline{\sigma}}_h) \in \mathbf{V}(\mathcal{T}_h)$, with the following error estimate:

$$|||(v_F - v_{Fh}, p - p_h, v_F - v_{Fh}, p - p_h)|||_{TDG} \leq$$
$$3 \inf_{(\omega_F, q, \omega_S, \underline{\underline{\xi}}) \in \mathbf{V}(\mathcal{T}_h)} |||(v_F - \omega_F, p - q, v_S - \omega_S, \underline{\underline{\sigma}} - \underline{\underline{\xi}})|||_{TDG^*}.$$

3 Implementation of the method

In this section we consider a simple example of seismic wave propagation in 1D homogeneous acoustic media with periodical and Dirichlet boundaries, in order to better understand a numerical implementation procedure. We introduce a rectangular space-time mesh, and a polynomial Trefftz space. We compare numerical results with exact solutions, and analyze the numerical error.

3.1 1D Acoustic system

We choose a space domain $\Omega_F \equiv [x_L, x_R]$ and a time domain $I \equiv [0, T]$ so that $Q_F \equiv \Omega_F \times I$ represents a rectangle. To avoid any difficulty related to the discretization of the boundary conditions, we consider first 1D AS in homogeneous media with periodical boundary conditions:

$$\begin{cases} \dfrac{1}{c_F^2}\dfrac{\partial p}{\partial t} + \dfrac{\partial v_F}{\partial x} = 0 \text{ in } Q_F, \\ \dfrac{\partial v_F}{\partial t} + \dfrac{\partial p}{\partial x} = 0 \text{ in } Q_F, \\ v_F(\cdot, 0) = v_{F0},\ p(\cdot, 0) = p_0 \text{ in } \Omega_F, \\ v_F(x_L, \cdot) = v_F(x_R, \cdot),\ p(x_L, \cdot) = p(x_R, \cdot) \text{ in } [0, T]. \end{cases} \tag{15}$$

3.1.1 Trefftz-DG formulation

The uniform mesh $\mathcal{T}_h$ on Q_F is composed of non-overlapping rectangular elements K_F^k, $k = 1, ..N_{el}$, $N_{el} = N_x \times N_t$, with edges parallel to the space and time axes, and equal to $\Delta x = (x_R - x_L)/N_x$ and $\Delta t = T/N_t$ respectively (see Figure 1). In Chapter 2.1, we have already proven well-posedness of Trefftz-DG variational problem for this type of mesh.

We recall the definition of Trefftz space:

$$\mathbf{T}_F(\mathcal{T}_h) \equiv \Big\{ (\omega_F, q) \subset H^1(\mathcal{T}_h)^2 \text{ s. t. } \frac{\partial \omega_F}{\partial t} + \frac{\partial q}{\partial x} = \frac{1}{c_F^2}\frac{\partial q}{\partial t} + \frac{\partial \omega_F}{\partial x} = 0 \text{ in all } K_F \in \mathcal{T}_h \Big\}.$$

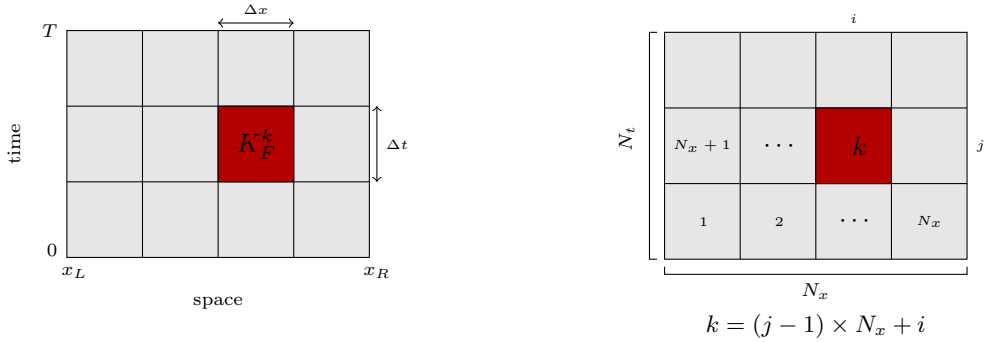

Figure 1: Uniform rectangular mesh $\mathcal{T}_h$ on Q_F. Element numbering.

Trefftz-DG formulation for (15) reads as:

Seek $(v_{Fh}, p_h) \subset \mathbf{V}(\mathcal{T}_h)$ *s.t. for all* $(\omega_F, q) \subset \mathbf{V}(\mathcal{T}_h)$ *it holds*

$$\begin{aligned}
&\int_{\mathcal{F}_h^{\Omega_F}} \Big[\frac{1}{c_F^2} p_h{}^- [\![q]\!]_t + v_{Fh}{}^- [\![\omega_F]\!]_t\Big] ds \\
&+ \int_{\mathcal{F}_h^{I_F}} \Big[\{p_h\}[\![\omega_F]\!]_x + \{v_{Fh}\}[\![q]\!]_x + \alpha [\![v_{Fh}]\!]_x [\![\omega_F]\!]_x + \beta [\![p_h]\!]_x [\![q]\!]_x\Big] ds \\
&+ \int_{\mathcal{F}_h^{T_F}} \Big[\frac{1}{c_F^2} p_h q + v_{Fh}\omega_F\Big] ds - \frac{1}{2}\int_{\mathcal{F}_h^{0_F}} \Big[\frac{1}{c_F^2} p_h q + v_{Fh}\omega_F\Big] ds = \\
&\frac{1}{2}\int_{\mathcal{F}_h^{0_F}} \Big[\frac{1}{c_F^2} p_h q + v_{Fh}\omega_F\Big] ds.
\end{aligned} \tag{16}$$

3.1.2 Numerical algorithm

Once we have defined the discrete approximation space, we can solve the problem inside each element K_F, communicating values at the boundaries ∂K_F by the in-coming and out-going fluxes. Thus, variational problem (16) will be represented by a global algebraic linear system, with global sparse matrix, of size equals to the total number of elements multiplied by the number of degrees of freedom per element ($N_t \times N_x \times \text{ndof}$). The inversion of a huge matrix, numerically speaking, is a very expensive process. In order to optimize the execution of the algorithm, we will solve (16) "layer by layer", considering final results, computed on the current time layer at time t, as initial values for the next layer at time $t + \Delta t$ (see Figure 2).

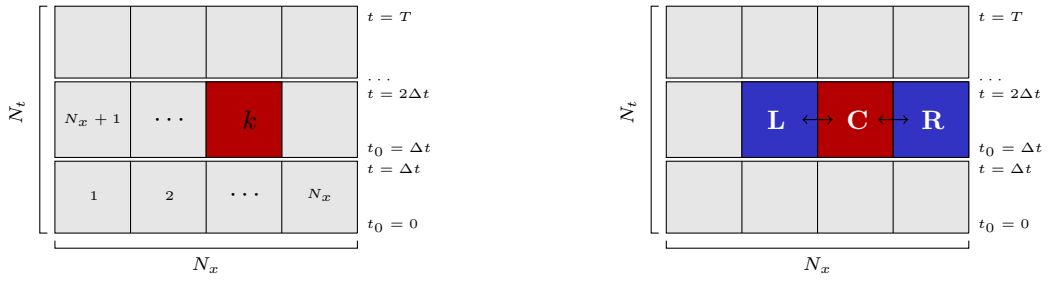

Figure 2: Uniform rectangular mesh $\mathcal{T}_h$ on Q_F. Decomposing on layers.

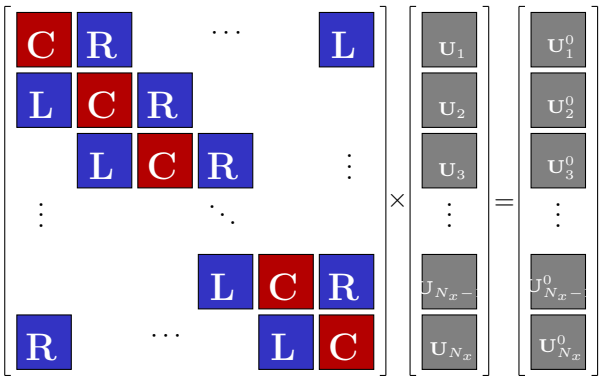

Figure 3: Global algebraic linear system with block tridiagonal matrix.

It means, that inside each time slab we solve the formulation inside each element, taking into account in-coming and out-going fluxes from its two neighbours (left and right ones). Thus, our matrix will have block tridiagonal form, of size N_t times smaller than the original one (see Figure 3).

One more feature to reduce numerical cost consists in computing space and time integrals on faces of one element of reference (unit square), and then, in projecting the computed values to all mesh elements (multiplying by Δx and Δt for space and time integration respectively in the case of rectangular mesh).

To sum up, we propose a short pseudo-code, which describes the algorithm of the method implementation.

```
Data: vt0, vp0                      % initial velocity and pressure fields
      c, rho, dx, dt, nx, nt        % medium and mesh parameters
Result: svfin, spfin                % final velocity and pressure fields
Compute:
v0=vinit(vt0)                       % velocity and pressure linear terms (t_0 = 0)
p0=pinit(pt0)
u0=0.5(v0+p0)                       % initial right-hand linear term
M                                   % global sparse matrix - left-hand bilinear term
invM = M^{-1}                       % inversion of the global matrix
for j = 1 : nt do
    Compute:
    u = invM*u0                     % vector of the coefficients for approximate solution
                                    % in the time slab [(j - 1) × dt, j × dt]
    svaux=vaux(u)                   % intermediate approximate solutions for
    spaux=paux(u)                   % velocity and pressure fields at time t_j = j × dt
    v0aux=vinit(vaux)               % intermediate velocity and pressure
    p0aux=pinit(paux)               % linear terms (t_j = j × dt)
    u0=0.5(v0aux+p0aux)             % reinitialization of the right-hand linear term
end
Compute:
svfin=vfin(u)                       % final approximate solutions for velocity
spfin=pfin(u)                       % and pressure fields at time t_nt = nt × dt
```

It is important to notice, that the main loop in time contains three steps: 1) computing the approximation coefficients of numerical solution in the current time slab; 2) computing the intermediate numerical solution using the approximation coefficients at the end of the current time slab; 3) reinitializing the initial values - computing the left-hand linear term at the beginning of the next time slab, using the intermediate numerical solutions from the previous step.

The idea to remove the last two steps, corresponding to the "projection" of the approximation coefficients to the numerical solution, is quite attractive, because it will provide faster execution of the code (we could reuse directly a vector of approximation coefficients computed in the previous slab). In order to explore this idea, we have used the algorithm based upon a high-order DG scheme, that arises after space semi-discretization of second order hyperbolic problems, proposed by Antonietti and Mazzieri in [27]. In this work, the authors derive an implicit arbitrarily high-order accurate time integration scheme based on DG spectral element approach. In contrast with finite difference time integration schemes, for which the solution at the current step depends upon the previous steps, time DG methods applied over time slabs $[t_j, t_{j+1}]$) lead to a casual system in which the solution at the current time slab depends only upon the solution at t_j^-. By coupling DG discretization in both space and time leads to a fully space-time finite element formulation.

In order to adapt the developed scheme to the method, described by the authors [27], we had

to replace the numerical fluxes $v_{\hat{F}h}$, $\hat{p_h}$ in (3) by central ones, to obtain completely symmetrical formulation. Numerical tests of this model with symmetrical formulation gave positive results in the case, when initial conditions and zero source term have been imposed. The case with a non-zero source is still under study.

3.1.3 Polynomial basis

Before presenting the numerical tests, we want to give an example of a polynomial Trefftz space. As we discussed in the previous sections, many choices of basis functions are possible. The main condition is to satisfy the Trefftz property inside each element. We have computed a polynomial basis, defined in the element of reference, using generating exponential functions - local solutions of initial 1D AS [26]. This basis contains the couples of polynomial functions $(\hat{\phi^v_.}, \hat{\phi^p_.})$, for velocity and pressure respectively, of degrees less or equal to p (p = 0, 1, 2, 3), satisfying the Trefftz property, to provide p^{th} approximation order (see Appendix B for more details):

$$\begin{array}{llll}
\phi^v_1 = 0 & \phi^v_2 = 1 & \phi^v_3 = x & \phi^v_4 = c_F t \\
\phi^p_1 = -c_F & \phi^p_2 = 0 & \phi^p_3 = -c_F^2 t & \phi^p_4 = -c_F x \\
\\
\phi^v_5 = -\frac{x^2}{2} - \frac{c_F^2 t^2}{2} & \phi^v_6 = -c_F x t & \phi^v_7 = -\frac{x^3}{6} - \frac{x c_F^2 t^2}{2} & \phi^v_8 = -\frac{c_F^3 t^3}{6} - \frac{x^2 c_F t}{2} \\
\phi^p_5 = c_F^2 x t & \phi^p_6 = c_F(\frac{x^2}{2} + \frac{c_F^2 t^2}{2}) & \phi^p_7 = c_F(\frac{c_F^3 t^3}{6} + \frac{x^2 c_F t}{2}) & \phi^p_8 = c_F(\frac{x^3}{6} + \frac{x c_F^2 t^2}{2}).
\end{array}$$

4 Numerical tests

The numerical test results are given in this Chapter for one- and two-dimensional models.

4.1 1D Acoustic simulations

We started with an example of wave propagation, caused by initial velocities and pressures, in absence of external forces. The acoustic media is represented by interval $\Omega_F \equiv [0,1]$, and the final time of propagation is $T = 1.0$. Periodical conditions are imposed at the boundaries. We set the media parameters $\rho_F = c_F = 1.0$. As the initial conditions, we consider two periodical functions: the "sin" function ($v_{F0} = sin(2\pi x)$ and $p_0 = -c_F v_{F0}$) and "hat" function ($v_{F0}(x) = 0$, $x \in [0, 1/3) \cup [2/3, 1]$, $v_{F0}(x) = x - 1/3$, $x \in [1/3, 1/2)$, $v_{F0}(x) = -x + 2/3$, $x \in [1/2, 2/3)$ and $p_0 = -c_F v_{F0}$). The model parameters are nondimensionalized.

Figures 5-7 show propagation of velocity v_F for initial "sin" (Figure 5) and "hat" (Figure 6-7) conditions, with different values of penalty parameters α and β. Figure (b) corresponds to the propagation in time of the numerical velocity. Figure (a) compares numerical (green) and exact (blue) velocities in the end of propagation at time $T = 1$ (one period).

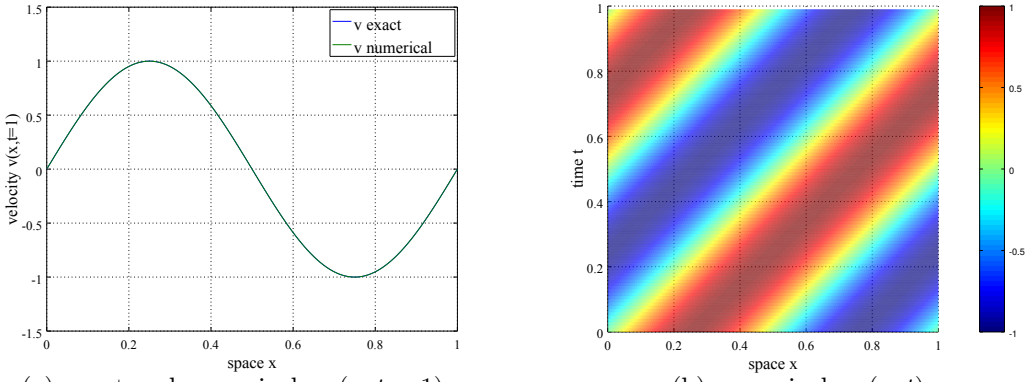

(a) exact and numerical $v_F(x, t = 1)$ (b) numerical $v_F(x, t)$

Figure 4: 1D AS ($\alpha = \beta = 0.0$). Propagation of velocity $v_F(x, t)$.

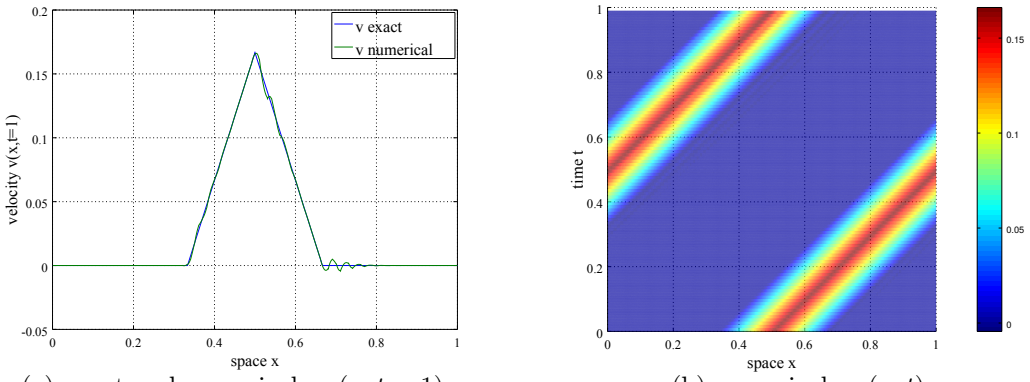

(a) exact and numerical $v_F(x, t = 1)$ (b) numerical $v_F(x, t)$

Figure 5: 1D AS ($\alpha = \beta = 0.0$). Propagation of velocity $v_F(x, t)$.

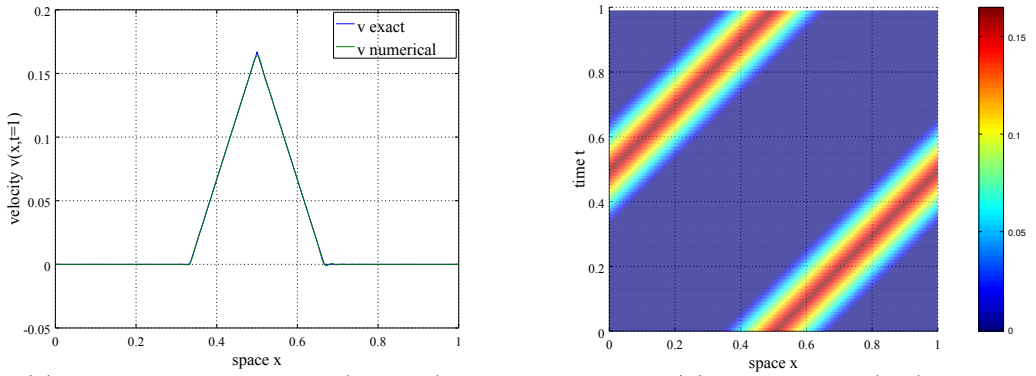

(a) exact and numerical $v_F(x, t = 1)$ (b) numerical $v_F(x, t)$

Figure 6: 1D AS ($\alpha = \beta = 0.5$). Propagation of velocity $v_F(x, t)$.

We can observe that in the "*sin*" test case, where initial wave is enough regular, the approximation works well even with penalty parameters $\alpha = \beta = 0$ (Figure 5). Although, if we chose the initial condition less regular ("*hat*" case), the numerical solution with zero penalty becomes less stable at the end of propagation (Figure 6), comparing to the case with $\alpha = \beta = 0.5$ (Figure 7).

Figure 8 shows some results of convergence of the velocity for zero (a) and non-zero (b) penalty parameters. The convergence curves have been computed for different approximation orders (p=0, 1, 2, 3), and they represent the numerical error as a function of cell size in logarithmic scale.

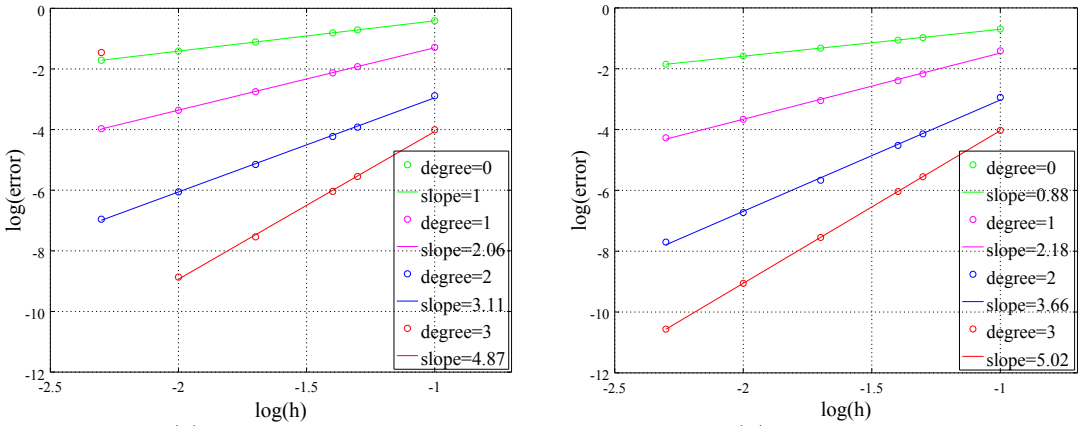

(a) $\alpha = \beta = 0.0$ (b) $\alpha = \beta = 0.5$

Figure 7: 1D AS. Convergence of velocity v_F in function of cell size $h = \Delta x$.

As we can see, convergence in both cases is of order higher, than corresponding approximation order. Moreover, the results are significantly better in the case of non-zero α and β.

The question of an optimal choice of penalty parameters is still open.

4.2 2D Simulations

In this section we present results obtained when applying the algorithm to the 2D acoustic, elastic, and elasto-acoustic problems.

We need to notice, that the currently developed code is a prototype MATLAB® version, which is, technically speaking, quite limited. This version has been created in order to explore the method and algorithm in general, and to perform some basic numerical tests for its validation.

The development of a new high-performance software must be the next step. It will require the implementation of new propagators based on libraries, which have already been developed on the Carbon platform by Magique-3D and Total.

Figure 9 shows some results of convergence of the velocity in two-dimensional acoustic (left) and elastodynamic (right) cases. The initial conditions are the plane waves - the exact solutions of 2D AS and ES. Space domain in both cases is represented by a unit square, time propagation $T = 1$. Medium parameters in acoustic media are $\rho_F = 1.0$, $c_F = 2.0$, in elastic media - $\rho_S = 1.0$, $\lambda = 1.0$, $\mu = 2.0$. As in previous example, the convergence curves have been computed for different approximation orders (p $= 0, 1, 2, 3$), and they represent the numerical error as a function of cell size in logarithmic scale.

Again, the convergence in both cases is of order higher, than corresponding approximation order.

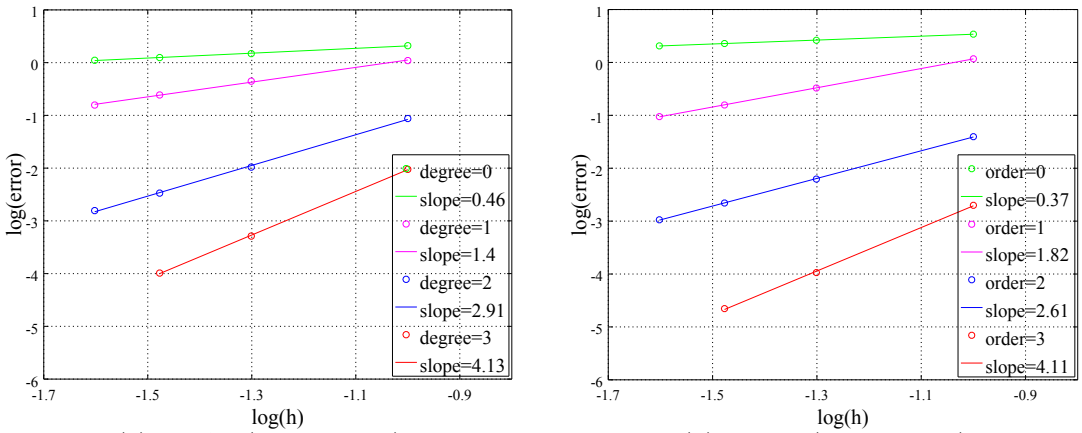

(a) 2D AS ($\alpha = \beta = 0.5$) (b) 2D ES ($\alpha = \beta = 0.5$)

Figure 8: Convergence of velocities v_F in acoustics and v_S in elastodynamics in function of cell size $h = \Delta x$.

Wave propagation in coupled elasto-acoustic media is represented by the snapshots in the Figure 10. The coupled fluid-solid medium is a unit square, and it contains two identical in form rectangular layers: acoustic on the top, and elastic at the bottom. Media parameters have been conserved from the previous tests. We consider zero initial conditions, and introduce a source term in the middle of the acoustic layer.

The source signal emitted at the source point src=(0.5,0.25) is represented by the first derivative of a Gaussian function, so that it takes approximately six elements per wavelength. Dirichlet conditions are imposed at the boundaries.

The character of propagation corresponds perfectly to physical expectations. Even if the model is limited (large mesh of $30 \times 30 \times 30$ elements, Dirichlet boundaries, which causes many reflections), we can observe all type of waves (P, S - waves, incident, reflected waves and waves of P, S - head waves).

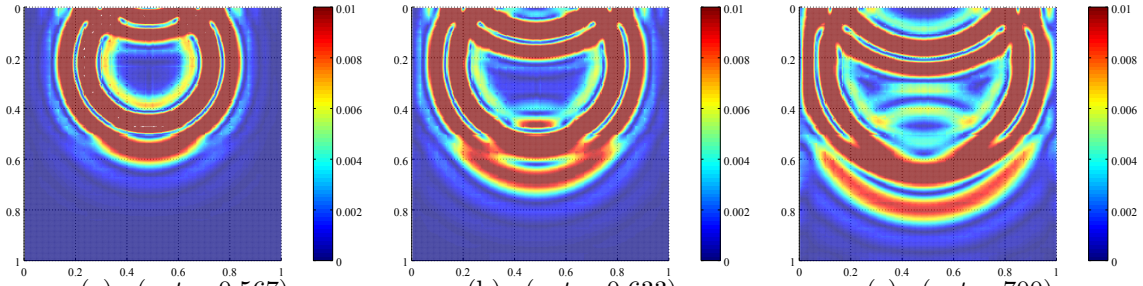

(a) $v(x, t = 0.567)$ (b) $v(x, t = 0.633)$ (c) $v(x, t = 700)$

Figure 9: 2D EAS ($\alpha = \beta = 0.5$). Propagation of numerical velocity $v(x, t)$.

In order to validate this test case, we have compared numerical signal measured at the receiver point rec=(0.65,0.70) with the analytical one, computed by the method of Cagniard de Hoop [12], using Gar6more2D [11] (see Figure 11).

We can observe that both signals are well-matched, conserving frequencies and amplitudes, There are still some imperfections, which are, probably, caused by the limited model.

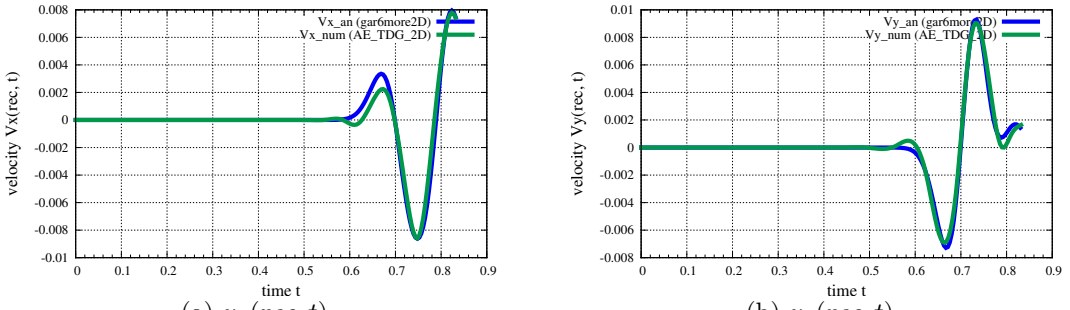

(a) $v_x(rec, t)$ (b) $v_y(rec, t)$

Figure 10: 2D EAS ($\alpha = \beta = 0.5$). Numerical and analytical seismograms for velosity $v(rec, t)$.

5 Conclusion

We have developed the theory of Trefftz-DG method applied to the coupled elasto-acoustic system, we have studied well-posedness of the problem, and proved error estimates in suitable mesh-dependent norms. The new polynomial basis has been computed for numerical implementation of the method. Currently, we have developed a prototype of MATLAB® code for 2D acoustic, elastodynamic, and elasto-acoustic problems, with implemented source term, Dirichlet boundary conditions and rectangular mesh. It has been validated by the analytical solutions. The convergence results are of higher order, compared to the classical DG methods. Moreover, Trefttz-DG variational formulation is simpler to compute, because it contains surface integration only, without any differential operators.

However, it is still early to discuss the performance of the code, before its optimization and paralleling. Thus, many directions are possible to explore, for both algorithmic and coding parts, such as: to continue studies of change-over between time layers in a case of implemented source [27], to study the optimal choice of penalty terms; to find the alternative to a global matrix inversion, which brings the main computational cost; to implement absorbing boundaries and perfectly matched layers for executing more proper simulations; to pass from simple rectangular meshes to more complicate (in space domain) forms - which is one of main advantages of Trefftz-DG methods. The last one gives the possibility of developing a hybrid method, based on numerical coupling of Trefftz-DG method in elastics, with less "expensive" finite volume method in acoustic media, in order to create more realistic software.

The work, presented in this report, is still under way. We have obtained very promising results, which deserve the development of a high-performance code, to be able to assess the method correctly.

A Mesh-dependent L^2-norm estimations

All estimations proposed in this Appendix are based on definitions and properties of the space and time normal jumps and average between elements [19], the Green's identities, and the symmetry of the stress and infinitesimal strain tensors [25].

A.1 Acoustic case

We consider the bilinear form $\mathcal{A}_{TDG_F}(\cdot;\cdot)$ in terms of test functions (ω_F, q):

$$\begin{aligned}
\mathcal{A}_{TDG_F}((\omega_F,q);(\omega_F,q)) \equiv & \int_{\mathcal{F}_h^{\Omega_F}} \Big[\frac{1}{c_F^2\rho_F} q^- [\![q]\!]_t + \rho_F {\omega_F}^- [\![\omega_F]\!]_t\Big] d\mathrm{s} \\
& + \int_{\mathcal{F}_h^{I_F}} \Big[\{\!\{q\}\!\}[\![\omega_F]\!]_x + \{\!\{\omega_F\}\!\}[\![q]\!]_x + \alpha[\![\omega_F]\!]_x^2 + \beta[\![q]\!]_x^2\Big] d\mathrm{s} \\
& + \int_{\mathcal{F}_h^{T_F}} \Big[\frac{1}{c_F^2\rho_F} q^2 + \rho_F\omega_F^2\Big] d\mathrm{s} - \frac{1}{2}\int_{\mathcal{F}_h^0} \Big[\frac{1}{c_F^2\rho_F} q^2 + \rho_F\omega_F^2\Big] d\mathrm{s} \\
& + \int_{\mathcal{F}_h^{D_F}} \Big[(q n_{K_F}^x + \alpha\omega_F)\cdot\omega_F\Big] d\mathrm{s} = \\
& \overbrace{\int_{\mathcal{F}_h^{\Omega_F}} \Big[\frac{1}{c_F^2\rho_F} q^- [\![q]\!]_t + \rho_F {\omega_F}^- [\![\omega_F]\!]_t\Big] d\mathrm{s}}^{[1]} \\
& + \overbrace{\int_{\mathcal{F}_h^{I_F}} \Big[\{\!\{q\}\!\}[\![\omega_F]\!]_x + \{\!\{\omega_F\}\!\}[\![q]\!]_x\Big] d\mathrm{s}}^{[2]} + \overbrace{\int_{\mathcal{F}_h^{I_F}} \Big[\alpha[\![\omega_F]\!]_x^2 + \beta[\![q]\!]_x^2\Big] d\mathrm{s}}^{[3]} \\
& + \overbrace{\frac{1}{2}\int_{\mathcal{F}_h^{T_F}} \Big[\frac{1}{c_F^2\rho_F} q^2 + \rho_F\omega_F^2\Big] d\mathrm{s} - \frac{1}{2}\int_{\mathcal{F}_h^{0_F}} \Big[\frac{1}{c_F^2\rho_F} q^2 + \rho_F\omega_F^2\Big] d\mathrm{s}}^{[4]} \\
& + \overbrace{\frac{1}{2}\int_{\mathcal{F}_h^{T_F}} \Big[\frac{1}{c_F^2\rho_F} q^2 + \rho_F\omega_F^2\Big] d\mathrm{s}}^{[5]} + \overbrace{\int_{\mathcal{F}_h^{D_F}} \alpha\omega_F^2 d\mathrm{s}}^{[6]} + \overbrace{\int_{\mathcal{F}_h^{D_F}} q n_{K_F}^x \cdot \omega_F d\mathrm{s}}^{[7]}.
\end{aligned}$$

Each member of the formulation above can be estimated in mesh-dependent L^2 norms as follows:

$$\begin{aligned}
[3] \equiv & \int_{\mathcal{F}_h^{I_F}} \Big[\alpha[\![\omega_F]\!]_x^2 + \beta[\![q]\!]_x^2\Big] d\mathrm{s} = \int_{\mathcal{F}_h^{I_F}} \Big[\alpha^{1/2}[\![\omega_F]\!]_x\Big]^2 d\mathrm{s} + \int_{\mathcal{F}_h^I} \Big[\beta^{1/2}[\![q]\!]_x\Big]^2 d\mathrm{s} = \\
& \Big\|\alpha^{1/2}[\![\omega_F]\!]_x\Big\|^2_{L^2(\mathcal{F}_h^{I_F})} + \Big\|\beta^{1/2}[\![q]\!]_x\Big\|^2_{L^2(\mathcal{F}_h^{I_F})};
\end{aligned}$$

$$\begin{aligned}
[5] \equiv & \frac{1}{2}\int_{\mathcal{F}_h^{T_F}} \Big[\frac{1}{c_F^2\rho_F} q^2 + \rho_F\omega_F^2\Big] d\mathrm{s} = \frac{1}{2}\int_{\mathcal{F}_h^T} \Big[\frac{1}{c_F^2\rho_F}^{1/2} q\Big]^2 d\mathrm{s} + \frac{1}{2}\int_{\mathcal{F}_h^T} \Big[\rho_F^{1/2}\omega_F\Big]^2 d\mathrm{s} = \\
& \frac{1}{2}\Big\|\frac{1}{c_F^2\rho_F}^{1/2} q\Big\|^2_{L^2(\mathcal{F}_h^{T_F})} + \frac{1}{2}\Big\|\rho_F^{1/2}\omega_F\Big\|^2_{L^2(\mathcal{F}_h^{T_F})};
\end{aligned}$$

$$[6] \equiv \int_{\mathcal{F}_h^{D_F}} \alpha\omega_F^2 d\mathrm{s} = \int_{\mathcal{F}_h^{D_F}} \left[\alpha^{1/2}\omega_F\right]^2 d\mathrm{s} = \left\|\alpha^{1/2}\omega_F\right\|^2_{L^2(\mathcal{F}_h^{D_F})};$$

$$[2]+[7] \equiv \int_{\mathcal{F}_h^{I_F}} \Big[\{\!\{q\}\!\}[\![\omega_F]\!]_x + \{\!\{\omega_F\}\!\}[\![q]\!]_x\Big] d\mathrm{s} + \int_{\mathcal{F}_h^{D_F}} q n^x_{K_F}\cdot\omega_F d\mathrm{s} = \int_{\mathcal{F}_h^{I_F}} [\![q\omega_F]\!]_x d\mathrm{s}$$
$$+ \int_{\mathcal{F}_h^{D_F}} (q\omega_F)\cdot n^x_{K_F} d\mathrm{s} = \sum_{K_F\in\mathcal{T}_h}\int_{K_F} \frac{\partial(q\omega_F)}{\partial x} d\mathrm{v};$$

$$[1] \equiv \int_{\mathcal{F}_h^{\Omega_F}} \Big[\frac{1}{c_F^2\rho_F} q^- [\![q]\!]_t + \rho_F \omega_F{}^- [\![\omega_F]\!]_t\Big] d\mathrm{s} = \int_{\mathcal{F}_h^{\Omega_F}} \frac{1}{c_F^2\rho_F}\Big[\frac{1}{2|n^t_{K_F}|}[\![q]\!]_t^2 + \frac{1}{2}[\![q^2]\!]_t\Big] d\mathrm{s}$$
$$+ \int_{\mathcal{F}_h^{\Omega_F}} \rho_F\Big[\frac{1}{2|n^t_{K_F}|}[\![\omega_F]\!]^2 + \frac{1}{2}[\![\omega_F^2]\!]_t\Big] d\mathrm{s} = \frac{1}{2}\int_{\mathcal{F}_h^{\Omega_F}} \Big[\frac{1}{c_F^2\rho_F}[\![q^2]\!]_t + \rho_F[\![\omega_F^2]\!]_t\Big] d\mathrm{s}$$
$$+ \frac{1}{2|n^t_{K_F}|}\Big\|\frac{1}{c_F^2\rho_F}^{1/2} q\Big\|^2_{L^2(\mathcal{F}_h^{\Omega_F})} + \frac{1}{2|n^t_{K_F}|}\Big\|\frac{1}{c_F^2\rho_F}^{1/2}\omega_F\Big\|^2_{L^2(\mathcal{F}_h^{\Omega_F})};$$

$$[4]+[1] \equiv \frac{1}{2}\int_{\mathcal{F}_h^{T_F}} \Big[\frac{1}{c_F^2\rho_F} q^2 + \rho_F\omega_F^2\Big] d\mathrm{s} - \frac{1}{2}\int_{\mathcal{F}_h^{0_F}} \Big[\frac{1}{c_F^2\rho_F} q^2 + \rho_F\omega_F^2\Big] d\mathrm{s}$$
$$+ \frac{1}{2}\int_{\mathcal{F}_h^{\Omega_F}} \Big[\frac{1}{c_F^2\rho_F}[\![q^2]\!]_t + \rho_F[\![\omega_F^2]\!]_t\Big] d\mathrm{s} + \frac{1}{2|n^t_{K_F}|}\Big\|\frac{1}{c_F^2\rho_F}^{1/2} q\Big\|^2_{L^2(\mathcal{F}_h^{\Omega_F})}$$
$$+ \frac{1}{2|n^t_{K_F}|}\Big\|\frac{1}{c_F^2\rho_F}^{1/2}\omega_F\Big\|^2_{L^2(\mathcal{F}_h^{\Omega_F})} = \frac{1}{2}\sum_{K_F\in\mathcal{T}_h}\int_{K_F}\frac{1}{c_F^2\rho_F}\frac{\partial q^2}{\partial t} d\mathrm{v} + \frac{1}{2}\sum_{K_F\in\mathcal{T}_h}\int_{K_F}\rho_F\frac{\partial\omega_F^2}{\partial t} d\mathrm{v}$$
$$+ \frac{1}{2|n^t_{K_F}|}\Big\|\frac{1}{c_F^2\rho_F}^{1/2} q\Big\|^2_{L^2(\mathcal{F}_h^{\Omega_F})} + \frac{1}{2|n^t_{K_F}|}\Big\|\frac{1}{c_F^2\rho_F}^{1/2}\omega_F\Big\|^2_{L^2(\mathcal{F}_h^{\Omega_F})};$$

$$[2]+[7]+[4]+[1] \equiv \sum_{K_F\in\mathcal{T}_h}\int_{K_F}\frac{\partial(q\omega_F)}{\partial x} d\mathrm{v} + \frac{1}{2}\sum_{K_F\in\mathcal{T}_h}\int_{K_F}\frac{1}{c_F^2\rho_F}\frac{\partial q^2}{\partial t} d\mathrm{v}$$
$$+ \frac{1}{2}\sum_{K_F\in\mathcal{T}_h}\int_{K_F}\rho_F\frac{\partial\omega_F^2}{\partial t} d\mathrm{v} + \frac{1}{2|n^t_{K_F}|}\Big\|\frac{1}{c_F^2\rho_F}^{1/2} q\Big\|^2_{L^2(\mathcal{F}_h^{\Omega_F})} + \frac{1}{2|n^t_{K_F}|}\Big\|\frac{1}{c_F^2\rho_F}^{1/2}\omega_F\Big\|^2_{L^2(\mathcal{F}_h^{\Omega_F})} =$$
$$\sum_{K_F\in\mathcal{T}_h}\int_{K_F}\Big[q\big(\overbrace{\frac{1}{c_F^2\rho_F}\frac{\partial q}{\partial t} + \frac{\partial\omega_F}{\partial x}}^{=0\text{ in }\mathbf{T}_F(\mathcal{T}_h)}\big)\Big] d\mathrm{v} + \sum_{K_F\in\mathcal{T}_h}\int_{K_F}\Big[\big(\overbrace{\rho_F\frac{\partial\omega_F}{\partial t} + \frac{\partial q}{\partial x}}^{=0\text{ in }\mathbf{T}_F(\mathcal{T}_h)}\big)\omega_F\Big] d\mathrm{v}$$
$$+ \frac{1}{2|n^t_{K_F}|}\Big\|\frac{1}{c_F^2\rho_F}^{1/2} q\Big\|^2_{L^2(\mathcal{F}_h^{\Omega_F})} + \frac{1}{2|n^t_{K_F}|}\Big\|\frac{1}{c_F^2\rho_F}^{1/2}\omega_F\Big\|^2_{L^2(\mathcal{F}_h^{\Omega_F})}.$$

Thus we obtain mesh-dependent L^2 estimate for the bilinear form $\mathcal{A}_{TDG_F}(\cdot;\cdot)$:

$$\begin{aligned}\mathcal{A}_{TDG_F}((\omega_F,q);(\omega_F,q)) \equiv & \frac{1}{2}\Big\|(\frac{1}{c_F^2\rho_F})^{1/2}[\![q]\!]_t\Big\|^2_{L^2(\mathcal{F}_h^{\Omega_F})} + \frac{1}{2}\Big\|\rho_F^{1/2}[\![\omega_F]\!]_t\Big\|^2_{L^2(\mathcal{F}_h^{\Omega_F})} \\ & + \Big\|\alpha^{1/2}[\![\omega_F]\!]_x\Big\|^2_{L^2(\mathcal{F}_h^{I_F})} + \Big\|\beta^{1/2}[\![q]\!]_x\Big\|^2_{L^2(\mathcal{F}_h^{I_F})} \\ & + \frac{1}{2}\Big\|(\frac{1}{c_F^2\rho_F})^{1/2}q\Big\|^2_{L^2(\mathcal{F}_h^{T_F})} + \frac{1}{2}\Big\|\rho_F^{1/2}\omega_F\Big\|^2_{L^2(\mathcal{F}_h^{T_F})} + \|\alpha^{1/2}\omega_F\|^2_{L^2(\mathcal{F}_h^{D_F})}.\end{aligned}$$

A.2 Elastodynamic case

We consider the bilinear form $\mathcal{A}_{TDG_S}(\cdot;\cdot)$ in terms of test functions $(\omega_S,\underline{\xi})$:

$$\begin{aligned}\mathcal{A}_{TDG_S}((\omega_S,\underline{\xi});(\omega_S,\underline{\xi})) \equiv & \int_{\mathcal{F}_h^{\Omega_S}}\Big[\underline{\underline{A}}\underline{\xi}^-[\![\underline{\xi}]\!]_t + \rho_S{\omega_S}^-[\![\omega_S]\!]_t\Big]d\mathrm{s} \\ & - \int_{\mathcal{F}_h^{I_S}}\Big[\{\!\{\underline{\xi}\}\!\}[\![\omega_S]\!]_x + \{\!\{\omega_S\}\!\}[\![\underline{\xi}]\!]_x - \delta[\![\underline{\xi}]\!]_x^2 - \gamma[\![\omega_S]\!]_x^2\Big]d\mathrm{s} \\ & + \int_{\mathcal{F}_h^{T_S}}\Big[\underline{\underline{A}}\underline{\xi}^2 + \rho_S\omega_S^2\Big]d\mathrm{s} - \frac{1}{2}\int_{\mathcal{F}_h^{0_S}}\Big[\underline{\underline{A}}\underline{\xi}^2 + \rho_S\omega_S^2\Big]d\mathrm{s} \\ & - \int_{\mathcal{F}_h^{D_S}}\Big[(\omega_S\cdot n_{K_S}^x)\underline{\xi} - \delta\underline{\xi}^2\Big]d\mathrm{s} = \\ & \overbrace{\int_{\mathcal{F}_h^{\Omega_S}}\Big[\underline{\underline{A}}\underline{\xi}^-[\![\underline{\xi}]\!]_t + \rho_S{\omega_S}^-[\![\omega_S]\!]_t\Big]d\mathrm{s}}^{[1]} \\ & \overbrace{-\int_{\mathcal{F}_h^{I_S}}\Big[\{\!\{\underline{\xi}\}\!\}[\![\omega_S]\!]_x + \{\!\{\omega_S\}\!\}[\![\underline{\xi}]\!]_x\Big]d\mathrm{s}}^{[2]} + \overbrace{\int_{\mathcal{F}_h^{I_S}}\Big[\delta[\![\underline{\xi}]\!]_x^2 + \gamma[\![\omega_S]\!]_x^2\Big]d\mathrm{s}}^{[3]} \\ & \overbrace{+\frac{1}{2}\int_{\mathcal{F}_h^{T_S}}\Big[\underline{\underline{A}}\underline{\xi}^2 + \rho_S\omega_S^2\Big]d\mathrm{s} - \frac{1}{2}\int_{\mathcal{F}_h^{0_S}}\Big[\underline{\underline{A}}\underline{\xi}^2 + \rho_S\omega_S^2\Big]d\mathrm{s}}^{[4]} \\ & \overbrace{+\frac{1}{2}\int_{\mathcal{F}_h^{T_S}}\Big[\underline{\underline{A}}\underline{\xi}^2 + \rho_S\omega_S^2\Big]d\mathrm{s}}^{[5]} + \overbrace{\int_{\mathcal{F}_h^{D_S}}\delta\underline{\xi}^2 d\mathrm{s}}^{[6]} - \overbrace{\int_{\mathcal{F}_h^{D_S}}\underline{\xi}(\omega_S\cdot n_{K_S}^x)d\mathrm{s}}^{[7]}.\end{aligned}$$

Each member of the formulation above can be estimated in mesh-dependent L^2 norms as follows:

$$\begin{aligned}[3] \equiv & \int_{\mathcal{F}_h^{I_S}}\Big[\delta[\![\underline{\xi}]\!]_x^2 + \gamma[\![\omega_S]\!]_x^2\Big]d\mathrm{s} = \int_{\mathcal{F}_h^{I_S}}\Big[\delta^{1/2}[\![\underline{\xi}]\!]_x\Big]^2 d\mathrm{s} + \int_{\mathcal{F}_h^{I_S}}\Big[\gamma^{1/2}[\![\omega_S]\!]_x\Big]^2 d\mathrm{s} = \\ & \Big\|\delta^{1/2}[\![\underline{\xi}]\!]_x\Big\|^2_{L^2(\mathcal{F}_h^{I_S})} + \Big\|\gamma^{1/2}[\![\omega_S]\!]_x\Big\|^2_{L^2(\mathcal{F}_h^{I_S})};\end{aligned}$$

$$\begin{aligned}[5] \equiv & \frac{1}{2}\int_{\mathcal{F}_h^{T_S}}\Big[\underline{\underline{A}}\underline{\xi}^2 + \rho_S\omega_S^2\Big]d\mathrm{s} = \frac{1}{2}\int_{\mathcal{F}_h^{T_S}}\Big[\underline{\underline{A}}^{1/2}\underline{\xi}\Big]^2 d\mathrm{s} + \frac{1}{2}\int_{\mathcal{F}_h^{T_S}}\Big[\rho_S^{1/2}\omega_S\Big]^2 d\mathrm{s} = \\ & \frac{1}{2}\Big\|\underline{\underline{A}}^{1/2}\underline{\xi}\Big\|^2_{L^2(\mathcal{F}_h^{T_S})} + \frac{1}{2}\Big\|\rho_S^{1/2}\omega_S\Big\|^2_{L^2(\mathcal{F}_h^{T_S})};\end{aligned}$$

$$[6] \equiv \int_{\mathcal{F}_h^{D_S}} \delta \underline{\underline{\xi}}^2 d\mathrm{s} = \int_{\mathcal{F}_h^{D_S}} \left[\delta^{1/2} \underline{\underline{\xi}}\right]^2 d\mathrm{s} = \left\|\delta^{1/2} \underline{\underline{\xi}}\right\|^2_{L^2(\mathcal{F}_h^{D_S})};$$

$$[2] + [7] \equiv -\int_{\mathcal{F}_h^{I_S}} \left[\{\omega_S\}[\![\underline{\underline{\xi}}]\!]_x + \{\underline{\underline{\xi}}\}[\![\omega_S]\!]_x\right] d\mathrm{s} - \int_{\mathcal{F}_h^{D_S}} \underline{\underline{\xi}} \omega_S \cdot n^x_{K_S} d\mathrm{s} = -\int_{\mathcal{F}_h^{I_S}} [\![\underline{\underline{\xi}} \omega_S]\!]_x d\mathrm{s}$$
$$- \int_{\mathcal{F}_h^{D_S}} (\underline{\underline{\xi}} \omega_S) \cdot n^x_{K_S} d\mathrm{s} = -\sum_{K_F \in \mathcal{T}_h} \int_{K_F} \frac{\partial (\underline{\underline{\xi}} \omega_S)}{\partial x} d\mathrm{v};$$

$$[1] \equiv \int_{\mathcal{F}_h^{\Omega_S}} \left[\underline{\underline{A}} \underline{\underline{\xi}}^- [\![\underline{\underline{\xi}}]\!]_t + \rho_S {\omega_S}^- [\![\omega_S]\!]_t\right] d\mathrm{s} = \int_{\mathcal{F}_h^{\Omega_S}} \frac{1}{c_F^2 \rho_F} \left[\frac{1}{2|n^t_{K_S}|} [\![\underline{\underline{\xi}}]\!]^2_t + \frac{1}{2} [\![\underline{\underline{\xi}}^2]\!]_t\right] d\mathrm{s}$$
$$+ \int_{\mathcal{F}_h^{\Omega_S}} \rho_S \left[\frac{1}{2|n^t_{K_S}|} [\![\omega_S]\!]^2 + \frac{1}{2} [\![\omega_S^2]\!]_t\right] d\mathrm{s} = \frac{1}{2} \int_{\mathcal{F}_h^{\Omega_S}} \left[\underline{\underline{A}} [\![\underline{\underline{\xi}}^2]\!]_t + \rho_S [\![\omega_S^2]\!]_t\right] d\mathrm{s}$$
$$+ \frac{1}{2|n^t_{K_S}|} \left\| \frac{1}{c_F^2 \rho_F}^{1/2} \underline{\underline{\xi}} \right\|^2_{L^2(\mathcal{F}_h^{\Omega_S})} + \frac{1}{2|n^t_{K_S}|} \left\| \frac{1}{c_F^2 \rho_F}^{1/2} \omega_S \right\|^2_{L^2(\mathcal{F}_h^{\Omega_S})};$$

$$[4] + [1] \equiv \frac{1}{2} \int_{\mathcal{F}_h^{T_S}} \left[\underline{\underline{A}} \underline{\underline{\xi}}^2 + \rho_S \omega_S^2\right] d\mathrm{s} - \frac{1}{2} \int_{\mathcal{F}_h^{0_S}} \left[\underline{\underline{A}} \underline{\underline{\xi}}^2 + \rho_S \omega_S^2\right] d\mathrm{s}$$
$$+ \frac{1}{2} \int_{\mathcal{F}_h^{\Omega_S}} \left[\underline{\underline{A}} [\![\underline{\underline{\xi}}^2]\!]_t + \rho_S [\![\omega_S^2]\!]_t\right] d\mathrm{s} + \frac{1}{2|n^t_{K_S}|} \left\| \underline{\underline{A}}^{1/2} \underline{\underline{\xi}} \right\|^2_{L^2(\mathcal{F}_h^{\Omega_S})}$$
$$+ \frac{1}{2|n^t_{K_S}|} \left\| \rho_S^{1/2} \omega_S \right\|^2_{L^2(\mathcal{F}_h^{\Omega_S})} = \frac{1}{2} \sum_{K_S \in \mathcal{T}_h} \int_{K_S} \underline{\underline{A}} \frac{\partial \underline{\underline{\xi}}^2}{\partial t} d\mathrm{v} + \frac{1}{2} \sum_{K_S \in \mathcal{T}_h} \int_{K_S} \rho_S \frac{\partial \omega_S^2}{\partial t} d\mathrm{v}$$
$$+ \frac{1}{2|n^t_{K_S}|} \left\| \underline{\underline{A}}^{1/2} \underline{\underline{\xi}} \right\|^2_{L^2(\mathcal{F}_h^{\Omega_S})} + \frac{1}{2|n^t_{K_S}|} \left\| \rho_S^{1/2} \omega_S \right\|^2_{L^2(\mathcal{F}_h^{\Omega_S})};$$

$$[2] + [7] + [4] + [1] \equiv \sum_{K_S \in \mathcal{T}_h} \int_{K_S} \frac{\partial (\underline{\underline{\xi}} \omega_S)}{\partial x} d\mathrm{v} + \frac{1}{2} \sum_{K_S \in \mathcal{T}_h} \int_{K_S} \underline{\underline{A}} \frac{\partial \underline{\underline{\xi}}^2}{\partial t} d\mathrm{v} + \frac{1}{2} \sum_{K_S \in \mathcal{T}_h} \int_{K_S} \rho_S \frac{\partial \omega_S^2}{\partial t} d\mathrm{v}$$
$$+ \frac{1}{2|n^t_{K_S}|} \left\| \underline{\underline{A}}^{1/2} \underline{\underline{\xi}} \right\|^2_{L^2(\mathcal{F}_h^{\Omega_S})} + \frac{1}{2|n^t_{K_S}|} \left\| \rho_S^{1/2} \omega_S \right\|^2_{L^2(\mathcal{F}_h^{\Omega_S})} = \sum_{K_S \in \mathcal{T}_h} \int_{K_S} \left[\underline{\underline{\xi}} \overbrace{\left(\underline{\underline{A}} \frac{\partial \underline{\underline{\xi}}}{\partial t} + \frac{\partial \omega_S}{\partial x}\right)}^{=0 \text{ in } \mathbf{T}_S(\mathcal{T}_h)}\right] d\mathrm{v}$$
$$+ \sum_{K_S \in \mathcal{T}_h} \int_{K_S} \left[\overbrace{\left(\rho_S \frac{\partial \omega_S}{\partial t} + \frac{\partial \underline{\underline{\xi}}}{\partial x}\right)}^{=0 \text{ in } \mathbf{T}_S(\mathcal{T}_h)} \omega_S\right] d\mathrm{v} + \frac{1}{2|n^t_{K_S}|} \left\| \underline{\underline{A}}^{1/2} \underline{\underline{\xi}} \right\|^2_{L^2(\mathcal{F}_h^{\Omega_S})} + \frac{1}{2|n^t_{K_S}|} \left\| \rho_S^{1/2} \omega_S \right\|^2_{L^2(\mathcal{F}_h^{\Omega_S})}.$$

Thus we obtain mesh-dependent L^2 estimate for the bilinear form $\mathcal{A}_{TDG_S}(\cdot;\cdot)$:

$$\begin{aligned}\mathcal{A}_{TDG_S}((\omega_S,\underline{\xi});(\omega_S,\underline{\xi})) \equiv & \frac{1}{2}\left\|(\underline{\underline{A}})^{1/2}[\![\underline{\xi}]\!]_t\right\|^2_{L^2(\mathcal{F}_h^{\Omega_S})} + \frac{1}{2}\left\|\rho_S^{1/2}[\![\omega_S]\!]_t\right\|^2_{L^2(\mathcal{F}_h^{\Omega_S})} \\ & + \left\|\delta^{1/2}[\![\underline{\xi}]\!]_x\right\|^2_{L^2(\mathcal{F}_h^{I_S})} + \left\|\gamma^{1/2}[\![\omega_S]\!]_x\right\|^2_{L^2(\mathcal{F}_h^{I_S})} \\ & + \frac{1}{2}\left\|(\underline{\underline{A}})^{1/2}\underline{\xi}\right\|^2_{L^2(\mathcal{F}_h^{T_S})} + \frac{1}{2}\left\|\rho_s^{1/2}\omega_S\right\|^2_{L^2(\mathcal{F}_h^{T_S})} + \|\delta^{1/2}\underline{\xi}\|^2_{L^2(\mathcal{F}_h^{D_S})}.\end{aligned}$$

A.3 Elasto-acoustic case

We consider the bilinear form $\mathcal{A}_{TDG}(\cdot;\cdot)$ for elasto-acoustic problem and trying to regroup its members in order to apply the fluid-solid transmission property:

$$\begin{aligned}\mathcal{A}_{TDG}((v_{Fh},p_h,v_{Sh},\underline{\sigma}_h);(\omega_F,q,\omega_S,\underline{\xi})) \equiv & \int_{\mathcal{F}_h^{\Omega_F}}\Big[\frac{1}{c_F^2\rho_F}p_h^{-}[\![q]\!]_t + \rho_F v_{Fh}^{-}[\![\omega_f]\!]_t\Big]d\mathrm{s} \\ & + \int_{\mathcal{F}_h^{I_F}}\Big[\{\!\{p_h\}\!\}[\![\omega_F]\!]_x + \{\!\{v_{Fh}\}\!\}[\![q]\!]_x + \alpha[\![v_{Fh}]\!]_x[\![\omega_F]\!]_x + \beta[\![p_h]\!]_x[\![q]\!]_x\Big]d\mathrm{s} \\ & + \int_{\mathcal{F}_h^{T_F}}\Big[\frac{1}{c_F^2\rho_F}p_hq + \rho_F v_{Fh}\cdot\omega_f\Big]d\mathrm{s} - \frac{1}{2}\int_{\mathcal{F}_h^{0_F}}\Big[\frac{1}{c_F^2\rho_F}p_hq + \rho_F v_{Fh}\cdot\omega_F\Big]d\mathrm{s} \\ & + \int_{\mathcal{F}_h^{D_F}}\Big[(pn_{K_F}^x + \alpha v_{Fh})\cdot\omega_F\Big]d\mathrm{s} \\ & + \int_{\mathcal{F}_h^{FS}}\Big[(p_hn_{K_F}^x + \alpha(v_{Fh}-v_{Sh})\cdot n_{K_F}^x)\cdot\omega_F + v_{Sh}\cdot n_{K_F}^x q\Big]d\mathrm{s} \\ & + \int_{\mathcal{F}_h^{\Omega_S}}\Big[\underline{\underline{A}}\,\underline{\sigma}_h^{-} : [\![\underline{\xi}]\!]_t + \rho_S v_{Sh}^{-}[\![\omega_S]\!]_t\Big]d\mathrm{s} \\ & - \int_{\mathcal{F}_h^{I_S}}\Big[\{\!\{\underline{\sigma}_h\}\!\}[\![\omega_S]\!]_x + \{\!\{v_{Sh}\}\!\}[\![\underline{\xi}]\!]_x - \gamma[\![v_{Sh}]\!]_x[\![\omega_S]\!]_x - \delta[\![\underline{\sigma}_h]\!]_x[\![\underline{\xi}]\!]_x\Big]d\mathrm{s} \\ & + \int_{\mathcal{F}_h^{T_S}}\Big[\underline{\underline{A}}\,\underline{\sigma}_h : \underline{\xi} + \rho_S v_{Sh}\cdot\omega_s\Big]d\mathrm{s} - \frac{1}{2}\int_{\mathcal{F}_h^{0_S}}\Big[\underline{\underline{A}}\,\underline{\sigma}_h : \underline{\xi} + \rho_S v_{Sh}\cdot\omega_s\Big]d\mathrm{s} \\ & - \int_{\mathcal{F}_h^{D_S}}\Big[(v_{Sh}\cdot n_{K_S}^x)\underline{\xi} - \delta\underline{\sigma}_h : \underline{\xi}\Big]d\mathrm{s} \\ & - \int_{\mathcal{F}_h^{FS}}\Big[(v_{Sh}\cdot n_{K_S}^x)\underline{\xi} - \delta(\underline{\sigma}_h n_{K_S}^x - p_hn_{K_S}^x)\underline{\xi} - pn_{K_S}^x\cdot\omega_S\Big]d\mathrm{s} = \\ & \int_{\mathcal{F}_h^{\Omega_F}}\Big[\frac{1}{c_F^2\rho_F}p_h^{-}[\![q]\!]_t + \rho_F v_{Fh}^{-}[\![\omega_F]\!]_t\Big]d\mathrm{s} \\ & + \int_{\mathcal{F}_h^{I_F}}\Big[\{\!\{p_h\}\!\}[\![\omega_F]\!]_x + \{\!\{v_{Fh}\}\!\}[\![q]\!]_x + \alpha[\![v_{Fh}]\!]_x[\![\omega_F]\!]_x + \beta[\![p_h]\!]_x[\![q]\!]_x\Big]d\mathrm{s} \\ & + \int_{\mathcal{F}_h^{T_F}}\Big[\frac{1}{c_F^2\rho_F}p_hq + \rho_F v_{Fh}\cdot\omega_F\Big]d\mathrm{s} - \frac{1}{2}\int_{\mathcal{F}_h^{0_F}}\Big[\frac{1}{c_F^2\rho_F}p_hq + \rho_F v_{Fh}\cdot\omega_F\Big]d\mathrm{s} \\ & + \int_{\mathcal{F}_h^{D_F}\cup\mathcal{F}_h^{FS}} p_hn_{K_F}^x\cdot\omega_F d\mathrm{s} + \int_{\mathcal{F}_h^{D_F}}\alpha v_{Fh}\cdot\omega_F d\mathrm{s} \\ & + \int_{\mathcal{F}_h^{\Omega_S}}\Big[\underline{\underline{A}}\,\underline{\sigma}_h^{-} : [\![\underline{\xi}]\!]_t + \rho_S v_{Sh}^{-}[\![\omega_S]\!]_t\Big]d\mathrm{s}\end{aligned}$$

$$
\begin{aligned}
&-\int_{\mathcal{F}_h^{I_S}}\Big[\{\!\{\underline{\underline{\sigma}}_h\}\!\}[\![\omega_S]\!]_x+\{\!\{v_{Sh}\}\!\}[\![\underline{\underline{\xi}}]\!]_x-\gamma[\![v_{Sh}]\!]_x[\![\omega_S]\!]_x-\delta[\![\underline{\underline{\sigma}}_h]\!]_x[\![\underline{\underline{\xi}}]\!]_x\Big]d\mathrm{s}\\
&+\int_{\mathcal{F}_h^{T_S}}\Big[\underline{\underline{A}}\,\underline{\underline{\sigma}}_h:\underline{\underline{\xi}}+\rho_S v_{Sh}\cdot\omega_S\Big]d\mathrm{s}-\frac{1}{2}\int_{\mathcal{F}_h^{0_S}}\Big[\underline{\underline{A}}\,\underline{\underline{\sigma}}_h:\underline{\underline{\xi}}+\rho_S v_{Sh}\cdot\omega_S\Big]d\mathrm{s}\\
&-\int_{\mathcal{F}_h^{D_S}\cup\mathcal{F}_h^{FS}}(v_{Sh}\cdot n^x_{K_S})\underline{\underline{\xi}}d\mathrm{s}+\int_{\mathcal{F}_h^{D_S}}\delta\underline{\underline{\sigma}}_h:\underline{\underline{\xi}}d\mathrm{s}+\int_{\mathcal{F}_h^{FS}}\delta(\underline{\underline{\sigma}}_h n^x_{K_S}-p_h n^x_{K_S})\underline{\underline{\xi}}d\mathrm{s}\\
&+\int_{\mathcal{F}_h^{FS}}\Big[\alpha(v_{Fh}\cdot n^x_{K_F}-v_{Sh}\cdot n^x_{K_F})\cdot\omega_F+v_{Sh}\cdot n^x_{K_F}q+\omega_S\cdot n^x_{K_S}p\Big]d\mathrm{s}.
\end{aligned}
$$

The fluid-solid transmission property must be valid for the test velocities and stresses. We apply it to the bilinear form $\mathcal{A}_{TDG}(\cdot;\cdot)$ written in terms of test functions $(\omega_F,q,\omega_S,\underline{\underline{\xi}})$, we obtain:

$$
\begin{aligned}
&\mathcal{A}_{TDG}((\omega_F,q,\omega_S,\underline{\underline{\xi}});(\omega_F,q,\omega_S,\underline{\underline{\xi}}))\equiv\\
&\overbrace{\int_{\mathcal{F}_h^{\Omega_F}}\Big[\frac{1}{c_F^2\rho_F}q^-[\![q]\!]_t+\rho_F{\omega_F}^-[\![\omega_F]\!]_t\Big]d\mathrm{s}}^{[1]}\\
&+\overbrace{\int_{\mathcal{F}_h^{I_F}}\Big[\{\!\{q\}\!\}[\![\omega_F]\!]_x+\{\!\{\omega_F\}\!\}[\![q]\!]_x\Big]d\mathrm{s}}^{[2]}+\overbrace{\int_{\mathcal{F}_h^{I_F}}\Big[\alpha[\![\omega_F]\!]_x^2+\beta[\![q]\!]_x^2\Big]d\mathrm{s}}^{[3]}\\
&+\overbrace{\frac{1}{2}\int_{\mathcal{F}_h^{T_F}}\Big[\frac{1}{c_F^2\rho_F}q^2+\rho_F\omega_f^2\Big]d\mathrm{s}-\frac{1}{2}\int_{\mathcal{F}_h^{0_F}}\Big[\frac{1}{c_F^2\rho_F}q^2+\rho_F\omega_F^2\Big]d\mathrm{s}}^{[4]}\\
&+\overbrace{\frac{1}{2}\int_{\mathcal{F}_h^{T_F}}\Big[\frac{1}{c_F^2\rho_F}q^2+\rho_F\omega_F^2\Big]d\mathrm{s}}^{[5]}+\overbrace{\int_{\mathcal{F}_h^{D_F}}\alpha\omega_F^2d\mathrm{s}}^{[6]}+\overbrace{\int_{\mathcal{F}_h^{D_F}\cup\mathcal{F}_h^{FS}}qn^x_{K_F}\cdot\omega_Fd\mathrm{s}}^{[7]}\\
&+\overbrace{\int_{\mathcal{F}_h^{\Omega_S}}\Big[\underline{\underline{A}}\underline{\underline{\xi}}^-[\![\underline{\underline{\xi}}]\!]_t+\rho_S{\omega_S}^-[\![\omega_S]\!]_t\Big]d\mathrm{s}}^{[1']}\\
&-\overbrace{\int_{\mathcal{F}_h^{I_S}}\Big[\{\!\{\underline{\underline{\xi}}\}\!\}[\![\omega_S]\!]_x+\{\!\{\omega_S\}\!\}[\![\underline{\underline{\xi}}]\!]_x\Big]d\mathrm{s}}^{[2']}+\overbrace{\int_{\mathcal{F}_h^{I_S}}\Big[\delta[\![\omega_S]\!]_x^2+\gamma[\![\underline{\underline{\xi}}]\!]_x^2\Big]d\mathrm{s}}^{[3']}\\
&+\overbrace{\frac{1}{2}\int_{\mathcal{F}_h^{T_S}}\Big[\underline{\underline{A}}\underline{\underline{\xi}}^2+\rho_S\omega_S^2\Big]d\mathrm{s}-\frac{1}{2}\int_{\mathcal{F}_h^{0_S}}\Big[\underline{\underline{A}}\underline{\underline{\xi}}^2+\rho_S\omega_S^2\Big]d\mathrm{s}}^{[4']}\\
&+\overbrace{\frac{1}{2}\int_{\mathcal{F}_h^{T_S}}\Big[\underline{\underline{A}}\underline{\underline{\xi}}^2+\rho_S\omega_S^2\Big]d\mathrm{s}}^{[5']}+\overbrace{\int_{\mathcal{F}_h^{D_S}}\delta\underline{\underline{\xi}}^2d\mathrm{s}}^{[6']}-\overbrace{\int_{\mathcal{F}_h^{D_S}\cup\mathcal{F}_h^{FS}}\omega_S\cdot n^x_{K_S}\underline{\underline{\xi}}d\mathrm{s}}^{[7']}\\
&+\overbrace{\int_{\mathcal{F}_h^{FS}}2\delta\underline{\underline{\xi}}^2d\mathrm{s}}^{[0]}.
\end{aligned}
$$

Taking into account previously obtained results for acoustic and elastodynamic cases, each member of the formulation above can be estimated in mesh-dependent L^2 norms as follows:

$$[6] \equiv \int_{\mathcal{F}_h^{D_F}} \alpha\omega_F^2 d\mathrm{s} = \left\| \alpha^{1/2}\omega_F \right\|^2_{L^2(\mathcal{F}_h^{D_F})};$$

$$[6'] \equiv \left\| \delta^{1/2} \underline{\underline{\xi}} \right\|^2_{L^2(\mathcal{F}_h^{D_S})};$$

$$[3] \equiv \int_{\mathcal{F}_h^{I_F}} \left[\alpha [\![\omega_F]\!]_x^2 + \beta [\![q]\!]_x^2 \right] d\mathrm{s} = \left\| \alpha^{1/2} [\![\omega_F]\!]_x \right\|^2_{L^2(\mathcal{F}_h^{I_F})} + \left\| \beta^{1/2} [\![q]\!]_x \right\|^2_{L^2(\mathcal{F}_h^{I_F})};$$

$$[3'] \equiv \int_{\mathcal{F}_h^{I_S}} \left[\delta [\![\underline{\underline{\xi}}]\!]_x^2 + \gamma [\![\omega_S]\!]_x^2 \right] d\mathrm{s} = \left\| \delta^{1/2} [\![\underline{\underline{\xi}}]\!]_x \right\|^2_{L^2(\mathcal{F}_h^{I_S})} + \left\| \gamma^{1/2} [\![\omega_s]\!]_x \right\|^2_{L^2(\mathcal{F}_h^{I_S})};$$

$$[5] \equiv \frac{1}{2} \int_{\mathcal{F}_h^{T_F}} \left[\frac{1}{c_F^2 \rho_F} q^2 + \rho_F \omega_f^2 \right] d\mathrm{s} = \frac{1}{2} \left\| \frac{1}{c_F^2 \rho_F}^{1/2} q \right\|^2_{L^2(\mathcal{F}_h^{T_F})} + \frac{1}{2} \left\| \rho_F^{1/2} \omega_F \right\|^2_{L^2(\mathcal{F}_h^{T_F})};$$

$$[5'] \equiv \frac{1}{2} \int_{\mathcal{F}_h^{T_S}} \left[\underline{\underline{A}} \underline{\underline{\xi}}^2 + \rho_S \omega_S^2 \right] d\mathrm{s} = \frac{1}{2} \left\| \underline{\underline{A}}^{1/2} \underline{\underline{\xi}} \right\|^2_{L^2(\mathcal{F}_h^{T_S})} + \frac{1}{2} \left\| \rho_S^{1/2} \omega_S \right\|^2_{L^2(\mathcal{F}_h^{T_S})};$$

$$[1] + [2] + [4] + [7] \equiv \sum_{K_F \in \mathcal{T}_h} \int_{K_F} \Big[q \big(\overbrace{\frac{1}{c_F^2 \rho_F} \frac{\partial q}{\partial t} + \frac{\partial \omega_F}{\partial x}}^{=0 \text{ in } \mathbf{T}(\mathcal{T}_h)} \big) + \omega_F \big(\overbrace{\rho_F \frac{\partial \omega_F}{\partial t} + \frac{\partial q}{\partial x}}^{=0 \text{ in } \mathbf{T}(\mathcal{T}_h)} \big) \Big] d\mathrm{v}$$
$$+ \frac{1}{2|n^t_{K_F}|} \left\| \frac{1}{c_F^2 \rho_F}^{1/2} q \right\|^2_{L^2(\mathcal{F}_h^{\Omega_F})} + \frac{1}{2|n^t_{K_F}|} \left\| \frac{1}{c_F^2 \rho_F}^{1/2} \omega_F \right\|^2_{L^2(\mathcal{F}_h^{\Omega_F})};$$

$$[1'] + [2'] + [4'] + [7'] \equiv \sum_{K_S \in \mathcal{T}_h} \int_{K_S} \Big[\underline{\underline{\xi}} \big(\overbrace{\underline{\underline{A}} \frac{\partial \underline{\underline{\xi}}}{\partial t} + \frac{\partial \omega_S}{\partial x}}^{=0 \text{ in } \mathbf{T}(\mathcal{T}_h)} \big) + \omega_s \big(\overbrace{\rho_S \frac{\partial \omega_S}{\partial t} + \frac{\partial \underline{\underline{\xi}}}{\partial x}}^{=0 \text{ in } \mathbf{T}(\mathcal{T}_h)} \big) \Big] d\mathrm{v}$$
$$+ \frac{1}{2|n^t_{K_S}|} \left\| \underline{\underline{A}}^{1/2} \underline{\underline{\xi}} \right\|^2_{L^2(\mathcal{F}_h^{\Omega_S})} + \frac{1}{2|n^t_{K_S}|} \left\| \rho_s^{1/2} \omega_S \right\|^2_{L^2(\mathcal{F}_h^{\Omega_S})};$$

$$[0] \equiv \int_{\mathcal{F}_h^{FS}} 2\delta \underline{\underline{\xi}}^2 d\mathrm{s} = 2 \left\| \delta^{1/2} \underline{\underline{\xi}} \right\|^2_{L^2(\mathcal{F}_h^{FS})}.$$

Thus we obtain mesh-dependent L^2 estimate for the bilinear form $\mathcal{A}_{TDG}(\cdot;\cdot)$:

$$\begin{aligned}
\mathcal{A}_{TDG}((\omega_F,q,\omega_S,\underline{\underline{\xi}});(\omega_F,q,\omega_S,\underline{\underline{\xi}})) \equiv\ & \frac{1}{2}\left\|\left(\frac{1}{c_F^2\rho_F}\right)^{1/2}[\![q]\!]_t\right\|^2_{L^2(\mathcal{F}_h^{\Omega_F})} + \frac{1}{2}\left\|\rho_F^{1/2}[\![\omega_F]\!]_t\right\|^2_{L^2(\mathcal{F}_h^{\Omega_F})} \\
&+ \left\|\alpha^{1/2}[\![\omega_F]\!]_x\right\|^2_{L^2(\mathcal{F}_h^{I_F})} + \left\|\beta^{1/2}[\![q]\!]_x\right\|^2_{L^2(\mathcal{F}_h^{I_F})} \\
&+ \frac{1}{2}\left\|\left(\frac{1}{c_F^2\rho_F}\right)^{1/2}q\right\|^2_{L^2(\mathcal{F}_h^{T_F})} + \frac{1}{2}\left\|\rho_F^{1/2}\omega_F\right\|^2_{L^2(\mathcal{F}_h^{T_F})} + \|\alpha^{1/2}\omega_F\|^2_{L^2(\mathcal{F}_h^{D_F})} \\
&+ \frac{1}{2}\left\|(\underline{\underline{A}})^{1/2}[\![\underline{\underline{\xi}}]\!]_t\right\|^2_{L^2(\mathcal{F}_h^{\Omega_S})} + \frac{1}{2}\left\|\rho_S^{1/2}[\![\omega_S]\!]_t\right\|^2_{L^2(\mathcal{F}_h^{\Omega_S})} \\
&+ \left\|\delta^{1/2}[\![\underline{\underline{\xi}}]\!]_x\right\|^2_{L^2(\mathcal{F}_h^{I_S})} + \left\|\gamma^{1/2}[\![\omega_S]\!]_x\right\|^2_{L^2(\mathcal{F}_h^{I_S})} \\
&+ \frac{1}{2}\left\|(\underline{\underline{A}})^{1/2}\underline{\underline{\xi}}\right\|^2_{L^2(\mathcal{F}_h^{T_S})} + \frac{1}{2}\left\|\rho_S^{1/2}\omega_S\right\|^2_{L^2(\mathcal{F}_h^{T_S})} + \|\delta^{1/2}\underline{\underline{\xi}}\|^2_{L^2(\mathcal{F}_h^{D_S})} \\
&+ 2\|\delta^{1/2}\underline{\underline{\xi}}\|^2_{L^2(\mathcal{F}_h^{FS})}.
\end{aligned}$$

B Wave polynomials

B.1 1D Acoustic system

Wave polynomials can be computed using the "generating functions" [26].

We consider 1D AS:

$$\frac{\partial p}{\partial t} + c_F^2 \frac{\partial v_F}{\partial x} = 0,$$
$$\frac{\partial v_F}{\partial t} + \frac{\partial p}{\partial x} = 0.$$

Using Fourrier method of separation of variables we obtain two solutions $g^v(x,t)$ and $g^p(x,t)$ which satisfy the initial AS when $a^2 = b^2$.

$$g^v(a,b,x,t) = e^{i(ax+bc_F t)},$$
$$g^p(a,b,x,t) = -c_F e^{i(bx+ac_F t)}.$$

We will consider them as the generating functions for wave polynomials for velocity and pressure respectively. We decompose both generating functions in Taylor series expansions as follows:

$$e^{i(ax+bc_F t)} = \sum_{n=0}^{\infty}\sum_{k=0}^{n} S^v_{n-k,k}(x,t)a^{n-k}b^k,$$
$$-c_F e^{i(bx+ac_F t)} = \sum_{n=0}^{\infty}\sum_{k=0}^{n} S^p_{n-k,k}(x,t)a^{n-k}b^k.$$

Here $S^v_{n-k,k}(x,t)$ and $S^p_{n-k,k}(x,t)$ are polynomials of variables x, t containing c_F. Replacing b^2 by a^2 in both series we obtain:

$$e^{i(ax+bc_F t)} = \sum_{n=0}^{\infty}\sum_{k=0,k<2}^{n} Q^v_{n-k,k}(x,t)a^{n-k}b^k,$$
$$-c_F e^{i(bx+ac_F t)} = \sum_{n=0}^{\infty}\sum_{k=0,k<2}^{n} Q^p_{n-k,k}(x,t)a^{n-k}b^k.$$

The real and imaginary parts of polynomials Q^v and Q^p satisfy the initial AS:

$$R^v_{n-k,k}(x,t) = \Re(Q^v_{n-k,k}(x,t)), \qquad I^v_{n-k,k}(x,t) = \Im(Q^v_{n-k,k}(x,t)),$$
$$R^p_{n-k,k}(x,t) = \Re(Q^p_{n-k,k}(x,t)), \qquad I^p_{n-k,k}(x,t) = \Im(Q^p_{n-k,k}(x,t)).$$

Varying the parameters k and n in the formulation above we obtain:

$$
\begin{array}{llll}
R^v_{00}=1 & I^v_{00}=0 & R^p_{00}=-c_F & I^p_{00}=0\\
R^v_{10}=0 & I^v_{10}=x & R^p_{10}=0 & I^p_{10}=-c_F^2t\\
R^v_{01}=0 & I^v_{01}=c_Ft & R^p_{01}=0 & I^p_{01}=-c_Fx
\end{array}
$$

$$
\begin{array}{llll}
R^v_{20}=-\frac{x^2}{2}-\frac{c_F^2t^2}{2} & I^v_{20}=0 & R^p_{20}=c_F(\frac{x^2}{2}+\frac{c_F^2t^2}{2}) & I^p_{20}=0\\
R^v_{11}=-c_Fxt & I^v_{11}=0 & R^p_{11}=c_F^2xt & I^p_{11}=0\\
R^v_{02}=0 & I^v_{02}=0 & R^p_{02}=0 & I^p_{02}=0
\end{array}
$$

$$
\begin{array}{llll}
R^v_{30}=0 & I^v_{30}=-\frac{x^3}{6}-\frac{xc_F^2t^2}{2} & R^p_{30}=0 & I^p_{30}=-c_Fx\\
R^v_{21}=0 & I^v_{21}=-\frac{c_F^3t^3}{6}-\frac{x^2c_Ft}{2} & R^p_{21}=0 & I^p_{21}=-c_F^2t\\
R^v_{12}=0 & I^v_{12}=0 & R^p_{12}=0 & I^p_{12}=c_F(\frac{c_F^3t^3}{6}+\frac{x^2c_Ft}{2})\\
R^v_{03}=0 & I^v_{03}=0 & R^p_{03}=0 & I^p_{03}=c_F(\frac{x^3}{6}+\frac{xc_F^2t^2}{2})
\end{array}
$$

Thus, we denote one-dimensional wave polynomial basis as follows (approximation order p=3):

$$
\begin{array}{llll}
\phi^v_1=0 & \phi^v_2=1 & \phi^v_3=x & \phi^v_4=c_Ft\\
\phi^v_5=-\frac{x^2}{2}-\frac{c_F^2t^2}{2} & \phi^v_6=-c_Fxt & \phi^v_7=-\frac{x^3}{6}-\frac{xc_F^2t^2}{2} & \phi^v_8=-\frac{c_F^3t^3}{6}-\frac{x^2c_Ft}{2}
\end{array}
$$

$$
\begin{array}{llll}
\phi^p_1=-c_F & \phi^p_2=0 & \phi^p_3=-c_F^2t & \phi^p_4=-c_Fx\\
\phi^p_5=c_F^2xt & \phi^p_6=c_F(\frac{x^2}{2}+\frac{c_F^2t^2}{2}) & \phi^p_5=c_F(\frac{c_F^3t^3}{6}+\frac{x^2c_Ft}{2}) & \phi^p_6=c_F(\frac{x^3}{6}+\frac{xc_F^2t^2}{2})
\end{array}
$$

Each couple $(\phi^v_i,\phi^p_i)_{i=1,..2p+2}$ satisfies the initial acoustic system, thus, corresponds to the definition of the Trefftz basis functions.

B.2 2D Acoustic system

Table 2: Wave polynomial basis for velocity $v_F = (v_F^x(x,y,t); v_F^y(x,y,t))^T$ and pressure $p = p(x,y,t)$ fields (order p=0,1,2,3).

p=0	**ndof=3**	
$\phi_1^{vx} = 0$	$\phi_1^{vy} = 0$	$\phi_1^p = -c_F$
$\phi_2^{vx} = 1$	$\phi_2^{vy} = 0$	$\phi_2^p = 0$
$\phi_3^{vx} = 0$	$\phi_3^{vy} = 1$	$\phi_3^p = 0$
p=1	**ndof=9**	
$\phi_4^{vx} = -t$	$\phi_4^{vy} = 0$	$\phi_4^p = x$
$\phi_5^{vx} = x$	$\phi_5^{vy} = 0$	$\phi_5^p = -c_F^2 t$
$\phi_6^{vx} = 0$	$\phi_6^{vy} = x$	$\phi_6^p = 0$
$\phi_7^{vx} = 0$	$\phi_7^{vy} = -t$	$\phi_7^p = y$
$\phi_8^{vx} = y$	$\phi_8^{vy} = 0$	$\phi_8^p = 0$
$\phi_9^{vx} = 0$	$\phi_9^{vy} = y$	$\phi_9^p = -c_F^2 t$
p=2	**ndof=18**	
$\phi_{10}^{vx} = -2xt$	$\phi_{10}^{vy} = 0$	$\phi_{10}^p = x^2 + c_F^2 t^2$
$\phi_{11}^{vx} = 0$	$\phi_{11}^{vy} = -2yt$	$\phi_{11}^p = y^2 + c_F^2 t^2$
$\phi_{12}^{vx} = -yt$	$\phi_{12}^{vy} = -xt$	$\phi_{12}^p = xy$
$\phi_{13}^{vx} = -\frac{xy}{c_F^2}$	$\phi_{13}^{vy} = -\frac{t^2}{2}$	$\phi_{13}^p = yt$
$\phi_{14}^{vx} = -\frac{t^2}{2}$	$\phi_{14}^{vy} = -\frac{xy}{c_F^2}$	$\phi_{14}^p = xt$
$\phi_{15}^{vx} = x^2$	$\phi_{15}^{vy} = -2xy$	$\phi_{15}^p = 0$
$\phi_{16}^{vx} = y^2$	$\phi_{16}^{vy} = 0$	$\phi_{16}^p = 0$
$\phi_{17}^{vx} = 0$	$\phi_{17}^{vy} = x^2$	$\phi_{17}^p = 0$
$\phi_{18}^{vx} = -2xy$	$\phi_{18}^{vy} = y^2$	$\phi_{18}^p = 0$
p=3	**ndof=30**	
$\phi_{19}^{vx} = -c_F^2 t^3 - 3x^2 t$	$\phi_{19}^{vy} = 0$	$\phi_{19}^p = x^3 + 3c_F^2 xt^2$
$\phi_{20}^{vx} = 0$	$\phi_{20}^{vy} = -c_F^2 t^3 - 3y^2 t$	$\phi_{20}^p = y^3 + 3c_F^2 yt^2$
$\phi_{21}^{vx} = -2xyt$	$\phi_{21}^{vy} = -\frac{c_F^2 t^3}{3} - x^2 t$	$\phi_{21}^p = x^2 y + c_F^2 yt^2$
$\phi_{22}^{vx} = -xt^2$	$\phi_{22}^{vy} = -\frac{x^2 y}{c_F^2}$	$\phi_{22}^p = \frac{c_F^2 t^3}{3} + x^2 t$
$\phi_{23}^{vx} = -\frac{c_F^2 t^3}{3} - y^2 t$	$\phi_{23}^{vy} = -2xyt$	$\phi_{23}^p = y^2 x + c_F^2 xt^2$
$\phi_{24}^{vx} = 0$	$\phi_{24}^{vy} = -\frac{y^3}{3c_F^2} - y^2 t$	$\phi_{24}^p = \frac{c_F^2 t^3}{3} + y^2 t$
$\phi_{25}^{vx} = -\frac{yt^2}{2}$	$\phi_{25}^{vy} = -\frac{xy^2}{2c_F^2} - \frac{xt^2}{2}$	$\phi_{25}^p = xyt$
$\phi_{26}^{vx} = x^3$	$\phi_{26}^{vy} = -3x^2 y$	$\phi_{26}^p = 0$
$\phi_{27}^{vx} = y^3$	$\phi_{27}^{vy} = 0$	$\phi_{27}^p = 0$
$\phi_{28}^{vx} = x^2 y$	$\phi_{28}^{vy} = -xy^2$	$\phi_{28}^p = 0$
$\phi_{29}^{vx} = xy^2$	$\phi_{29}^{vy} = -\frac{y^3}{3}$	$\phi_{29}^p = 0$
$\phi_{30}^{vx} = 0$	$\phi_{30}^{vy} = x^3$	$\phi_{30}^p = 0$

B.3 2D Elastodynamic system

Table 3: Wave polynomial basis for velocity $v_S = (v_S^x(x,y,t); v_S^y(x,y,t))^T$ and pressure $\sigma = (\sigma_{xx}(x,y,t), \sigma_{yy}(x,y,t), \sigma_{xy}(x,y,t))$ fields (order p=0,1,2,3).

p=0	**ndof=5**			
$\phi_1^{vx} = 1$	$\phi_1^{vy} = 0$	$\phi_1^{\sigma xx} = 0$	$\phi_1^{\sigma yy} = 0$	$\phi_1^{\sigma xy} = 0$
$\phi_2^{vx} = 0$	$\phi_2^{vy} = 1$	$\phi_2^{\sigma xx} = 0$	$\phi_2^{\sigma yy} = 0$	$\phi_2^{\sigma xy} = 0$
$\phi_3^{vx} = 0$	$\phi_3^{vy} = 0$	$\phi_3^{\sigma xx} = 1$	$\phi_3^{\sigma yy} = 0$	$\phi_3^{\sigma xy} = 0$
$\phi_4^{vx} = 0$	$\phi_4^{vy} = 0$	$\phi_4^{\sigma xx} = 0$	$\phi_4^{\sigma yy} = 1$	$\phi_4^{\sigma xy} = 0$
$\phi_5^{vx} = 0$	$\phi_5^{vy} = 0$	$\phi_5^{\sigma xx} = 0$	$\phi_5^{\sigma yy} = 0$	$\phi_5^{\sigma xy} = 0$
p=1	**ndof=15**			
$\phi_6^{vx} = -y$	$\phi_6^{vy} = x$	$\phi_6^{\sigma xx} = 0$	$\phi_6^{\sigma yy} = 0$	$\phi_6^{\sigma xy} = 0$
$\phi_7^{vx} = t$	$\phi_7^{vy} = 0$	$\phi_7^{\sigma xx} = x$	$\phi_7^{\sigma yy} = 0$	$\phi_7^{\sigma xy} = 0$
$\phi_8^{vx} = 0$	$\phi_8^{vy} = 0$	$\phi_8^{\sigma xx} = y$	$\phi_8^{\sigma yy} = 0$	$\phi_8^{\sigma xy} = 0$
$\phi_9^{vx} = a_{11}x + 2a_{13}y$	$\phi_9^{vy} = a_{12}y$	$\phi_9^{\sigma xx} = t$	$\phi_9^{\sigma yy} = 0$	$\phi_9^{\sigma xy} = 0$
$\phi_{10}^{vx} = 0$	$\phi_{10}^{vy} = 0$	$\phi_{10}^{\sigma xx} = 0$	$\phi_{10}^{\sigma yy} = x$	$\phi_{10}^{\sigma xy} = 0$
$\phi_{11}^{vx} = 0$	$\phi_{11}^{vy} = t$	$\phi_{11}^{\sigma xx} = 0$	$\phi_{11}^{\sigma yy} = y$	$\phi_{11}^{\sigma xy} = 0$
$\phi_{12}^{vx} = a_{12}x + 2a_{23}y$	$\phi_{12}^{vy} = a_{22}y$	$\phi_{12}^{\sigma xx} = 0$	$\phi_{12}^{\sigma yy} = t$	$\phi_{12}^{\sigma xy} = 0$
$\phi_{13}^{vx} = 0$	$\phi_{13}^{vy} = 0$	$\phi_{13}^{\sigma xx} = 0$	$\phi_{13}^{\sigma yy} = 0$	$\phi_{13}^{\sigma xy} = x$
$\phi_{14}^{vx} = t$	$\phi_{14}^{vy} = 0$	$\phi_{14}^{\sigma xx} = 0$	$\phi_{14}^{\sigma yy} = 0$	$\phi_{14}^{\sigma xy} = y$
$\phi_{15}^{vx} = a_{13}x + 2a_{33}y$	$\phi_{15}^{vy} = a_{23}y$	$\phi_{15}^{\sigma xx} = 0$	$\phi_{15}^{\sigma yy} = 0$	$\phi_{15}^{\sigma xy} = t$
p=2	**ndof=30**			
$\phi_{16}^{vx} = 0$	$\phi_{16}^{vy} = 0$	$\phi_{16}^{\sigma xx} = y^2$	$\phi_{16}^{\sigma yy} = 0$	$\phi_{16}^{\sigma xy} = 0$
$\phi_{17}^{vx} = 2a_{11}xt$	$\phi_{17}^{vy} = 4a_{13}xt + 2a_{12}yt$	$\phi_{17}^{\sigma xx} = a_{11}x^2 + t^2$	$\phi_{17}^{\sigma yy} = a_{12}y^2$	$\phi_{17}^{\sigma xy} = 2a_{13}x^2$
$\phi_{18}^{vx} = yt$	$\phi_{18}^{vy} = -xt$	$\phi_{18}^{\sigma xx} = xy$	$\phi_{18}^{\sigma yy} = -xy$	$\phi_{18}^{\sigma xy} = 0$
$\phi_{19}^{vx} = \frac{a_{11}x^2}{2} - \frac{a_{12}y^2}{2} + \frac{t^2}{2}$	$\phi_{19}^{vy} = a_{13}x^2 + a_{12}y^2$	$\phi_{19}^{\sigma xx} = xt$	$\phi_{19}^{\sigma yy} = 0$	$\phi_{19}^{\sigma xy} = 0$
$\phi_{20}^{vx} = a_{13}y^2 + a_{11}xy$	$\phi_{20}^{vy} = -\frac{a_{11}x^2}{2} + \frac{a_{12}y^2}{2}$	$\phi_{20}^{\sigma xx} = yt$	$\phi_{20}^{\sigma yy} = 0$	$\phi_{20}^{\sigma xy} = 0$
$\phi_{21}^{vx} = 0$	$\phi_{21}^{vy} = 0$	$\phi_{21}^{\sigma xx} = 0$	$\phi_{21}^{\sigma yy} = x^2$	$\phi_{21}^{\sigma xy} = 0$
$\phi_{22}^{vx} = 2a_{12}xt$	$\phi_{22}^{vy} = 4a_{23}xt + 2a_{22}yt$	$\phi_{22}^{\sigma xx} = a_{12}x^2$	$\phi_{22}^{\sigma yy} = a_{22}y^2 + t^2$	$\phi_{22}^{\sigma xy} = 2a_{23}x^2$
$\phi_{23}^{vx} = 0$	$\phi_{23}^{vy} = 0$	$\phi_{23}^{\sigma xx} = 0$	$\phi_{23}^{\sigma yy} = xy$	$\phi_{23}^{\sigma xy} = -\frac{x^2}{2}$
$\phi_{24}^{vx} = \frac{a_{12}x^2}{2} - \frac{a_{22}y^2}{2}$	$\phi_{24}^{vy} = a_{23}x^2 + a_{22}xy$	$\phi_{24}^{\sigma xx} = 0$	$\phi_{24}^{\sigma yy} = xt$	$\phi_{24}^{\sigma xy} = 0$
$\phi_{25}^{vx} = a_{23}y^2 + a_{12}xy$	$\phi_{25}^{vy} = -\frac{a_{12}x^2}{2} + \frac{a_{22}y^2}{2} + \frac{t^2}{2}$	$\phi_{25}^{\sigma xx} = 0$	$\phi_{25}^{\sigma yy} = yt$	$\phi_{25}^{\sigma xy} = 0$
$\phi_{26}^{vx} = 2yt$	$\phi_{26}^{vy} = -2xt$	$\phi_{26}^{\sigma xx} = 0$	$\phi_{26}^{\sigma yy} = 0$	$\phi_{26}^{\sigma xy} = -x^2 + y^2$
$\phi_{27}^{vx} = 2a_{13}xt$	$\phi_{27}^{vy} = 4a_{33}xt + 2a_{23}yt$	$\phi_{27}^{\sigma xx} = a_{13}x^2$	$\phi_{27}^{\sigma yy} = a_{23}y^2$	$\phi_{27}^{\sigma xy} = 2a_{33}x^2 + t^2$
$\phi_{28}^{vx} = 0$	$\phi_{28}^{vy} = 0$	$\phi_{28}^{\sigma xx} = -\frac{x^2}{2}$	$\phi_{28}^{\sigma yy} = -\frac{y^2}{2}$	$\phi_{28}^{\sigma xy} = xy$
$\phi_{29}^{vx} = \frac{a_{13}x^2}{2} - \frac{a_{23}y^2}{2}$	$\phi_{29}^{vy} = a_{33}x^2 + a_{23}xy + \frac{t^2}{2}$	$\phi_{29}^{\sigma xx} = 0$	$\phi_{29}^{\sigma yy} = 0$	$\phi_{29}^{\sigma xy} = xt$
$\phi_{30}^{vx} = a_{33}y^2 + a_{13}xy + \frac{t^2}{2}$	$\phi_{30}^{vy} = -\frac{a_{13}x^2}{2} + \frac{a_{23}y^2}{2}$	$\phi_{30}^{\sigma xx} = 0$	$\phi_{30}^{\sigma yy} = 0$	$\phi_{30}^{\sigma xy} = yt$

p=3 **ndof=50**

$$\phi_{31}^{vx} = x^3 + 3(\lambda+2\mu)t^2x \quad \phi_{31}^{vy} = 0 \quad \phi_{31}^{\sigma xx} = (\lambda+2\mu)^2t^3 + 3(\lambda+2\mu)x^2t \quad \phi_{31}^{\sigma yy} = \lambda(\lambda+2\mu)t^3 + 3\lambda x^2t \quad \phi_{31}^{\sigma xy} = 0$$

$$\phi_{32}^{vx} = y^3 + 3\mu t^2y \quad \phi_{32}^{vy} = 0 \quad \phi_{32}^{\sigma xx} = 0 \quad \phi_{32}^{\sigma yy} = 0 \quad \phi_{32}^{\sigma xy} = \mu^2t^3 + 3\mu y^2t$$

$$\phi_{33}^{vx} = x^2y + (\lambda+2\mu)t^2y \quad \phi_{33}^{vy} = (\lambda+\mu)t^2x \quad \phi_{33}^{\sigma xx} = 2(\lambda+2\mu)xyt \quad \phi_{33}^{\sigma yy} = 2\lambda xyt \quad \phi_{33}^{\sigma xy} = \frac{\mu(2\lambda+3\mu)t^3}{3} + \mu x^2t$$

$$\phi_{34}^{vx} = \frac{(\lambda+2\mu)t^3}{3} + x^2t \quad \phi_{34}^{vy} = 0 \quad \phi_{34}^{\sigma xx} = (\lambda+2\mu)t^2x \quad \phi_{34}^{\sigma yy} = -y^2x + \lambda t^2x \quad \phi_{34}^{\sigma xy} = x^2y$$

$$\phi_{35}^{vx} = y^2x + \mu t^2x \quad \phi_{35}^{vy} = (\lambda+\mu)t^2y \quad \phi_{35}^{\sigma xx} = \frac{(m(\lambda+2\mu)+\lambda(\lambda+\mu))t^3}{3} + (\lambda+2\mu)y^2t \quad \phi_{35}^{\sigma yy} = \frac{((\lambda+\mu)(\lambda+2\mu)+\lambda\mu)t^3}{3} + \lambda y^2t \quad \phi_{35}^{\sigma xy} = 2\mu xyt$$

$$\phi_{36}^{vx} = \frac{\mu t^3}{3} + y^2t \quad \phi_{36}^{vy} = 0 \quad \phi_{36}^{\sigma xx} = y^2x \quad \phi_{36}^{\sigma yy} = 0 \quad \phi_{36}^{\sigma xy} = \mu t^2y$$

$$\phi_{37}^{vx} = xyt \quad \phi_{37}^{vy} = \frac{(\lambda+\mu)t^3}{6} \quad \phi_{37}^{\sigma xx} = \frac{x^2y}{2} + \frac{(\lambda+2\mu)t^2y}{2} \quad \phi_{37}^{\sigma yy} = \frac{t^2y}{2} \quad \phi_{37}^{\sigma xy} = \frac{\mu t^2x}{2}$$

$$\phi_{38}^{vx} = 0 \quad \phi_{38}^{vy} = x^3 + 3\mu t^2x \quad \phi_{38}^{\sigma xx} = 0 \quad \phi_{38}^{\sigma yy} = 0 \quad \phi_{38}^{\sigma xy} = \mu^2t^3 + 3\mu x^2t$$

$$\phi_{39}^{vx} = 0 \quad \phi_{39}^{vy} = y^3 + 3(\lambda+2\mu)t^2y \quad \phi_{39}^{\sigma xx} = l(\lambda+2\mu)t^3 + 3\lambda y^2t \quad \phi_{39}^{\sigma yy} = (\lambda+2\mu)^2t^3 + 3(\lambda+2\mu)y^2t \quad \phi_{39}^{\sigma xy} = 0$$

$$\phi_{40}^{vx} = (\lambda+\mu)t^2x \quad \phi_{40}^{vy} = x^2y + \mu t^2y \quad \phi_{40}^{\sigma xx} = \frac{((\lambda+\mu)(\lambda+2\mu)+\lambda\mu)t^3}{3} + \lambda x^2t \quad \phi_{40}^{\sigma yy} = \frac{(\mu(\lambda+2\mu)+\lambda(\lambda+\mu))t^3}{3} + (\lambda+2\mu)x^2t \quad \phi_{40}^{\sigma xy} = 2\mu xyt$$

$$\phi_{41}^{vx} = 0 \quad \phi_{41}^{vy} = \frac{\mu t^3}{3} + x^2t \quad \phi_{41}^{\sigma xx} = 0 \quad \phi_{41}^{\sigma yy} = x^2y \quad \phi_{41}^{\sigma xy} = \mu t^2x$$

$$\phi_{42}^{vx} = (\lambda+\mu)t^2y \quad \phi_{42}^{vy} = y^2x + (\lambda+2\mu)t^2x \quad \phi_{42}^{\sigma xx} = 2\lambda xyt \quad \phi_{42}^{\sigma yy} = 2(\lambda+2\mu)xyt \quad \phi_{42}^{\sigma xy} = \frac{\mu(2\lambda+3\mu)t^3}{3} + \mu y^2t$$

$$\phi_{43}^{vx} = 0 \quad \phi_{43}^{vy} = \frac{(\lambda+2\mu)t^3}{3} + y^2t \quad \phi_{43}^{\sigma xx} = -x^2y + \lambda t^2y \quad \phi_{43}^{\sigma yy} = (\lambda+2\mu)t^2y \quad \phi_{43}^{\sigma xy} = y^2x$$

$$\phi_{44}^{vx} = \frac{(\lambda+\mu)t^3}{6} \quad \phi_{44}^{vy} = xyt \quad \phi_{44}^{\sigma xx} = \frac{\lambda t^2x}{2} \quad \phi_{44}^{\sigma yy} = \frac{y^2x}{2} + \frac{(\lambda+2\mu)t^2x}{2} \quad \phi_{44}^{\sigma xy} = \frac{\mu t^2y}{2}$$

$$\phi_{45}^{vx} = 0 \quad \phi_{45}^{vy} = 0 \quad \phi_{45}^{\sigma xx} = x^3 \quad \phi_{45}^{\sigma yy} = 3y^2x \quad \phi_{45}^{\sigma xy} = 3x^2y$$

$$\phi_{46}^{vx} = 0 \quad \phi_{46}^{vy} = 0 \quad \phi_{46}^{\sigma xx} = y^3 \quad \phi_{46}^{\sigma yy} = 0 \quad \phi_{46}^{\sigma xy} = 0$$

$$\phi_{47}^{vx} = 0 \quad \phi_{47}^{vy} = 0 \quad \phi_{47}^{\sigma xx} = 0 \quad \phi_{47}^{\sigma yy} = x^3 \quad \phi_{47}^{\sigma xy} = 0$$

$$\phi_{48}^{vx} = 0 \quad \phi_{48}^{vy} = 0 \quad \phi_{48}^{\sigma xx} = 3x^2y \quad \phi_{48}^{\sigma yy} = y^3 \quad \phi_{48}^{\sigma xy} = -3y^2x$$

$$\phi_{49}^{vx} = 0 \quad \phi_{49}^{vy} = 0 \quad \phi_{49}^{\sigma xx} = 0 \quad \phi_{49}^{\sigma yy} = -3x^2y \quad \phi_{49}^{\sigma xy} = x^3$$

$$\phi_{50}^{vx} = 0 \quad \phi_{50}^{vy} = 0 \quad \phi_{50}^{\sigma xx} = -3xy^2 \quad \phi_{50}^{\sigma yy} = 0 \quad \phi_{50}^{\sigma xy} = y^3$$

Contents

References

[1] Keiiti Aki and Paul G Richards. *Quantitative seismology*. 2002.

[2] Ivo Babuška and Miloš Zlámal. Nonconforming elements in the finite element method with penalty. *SIAM Journal on Numerical Analysis*, 10(5):863–875, 1973.

[3] Zsolt Badics. Trefftz-discontinuous Galerkin and finite element multi-solver technique for modeling time-harmonic EM problems with high-conductivity regions. *IEEE Transactions on Magnetics*, 50(2):401–404, 2014.

[4] Caroline Baldassari, Hélene Barucq, Henri Calandra, Bertrand Denel, and Julien Diaz. Performance analysis of a high-order Discontinuous Galerkin method application to the reverse time migration. *Communications in Computational Physics*, 11(2):660–673, 2012.

[5] Lehel Banjai, Emmanuil H Georgoulis, and Oluwaseun Lijoka. A trefftz polynomial space-time discontinuous galerkin method for the second order wave equation. *SIAM Journal on Numerical Analysis*, 55(1):63–86, 2017.

[6] Hélène Barucq, Julien Diaz, Rabia Djellouli, and Elodie Estecahandy. High-order Discontinuous Galerkin approximations for elasto-acoustic scattering problems. 2015.

[7] F Bassi, S Rebay, G Mariotti, Savini Pedinotti, and M Savini. A high-order accurate discontinuous finite element method for inviscid and viscous turbomachinery flows. pages 99–109, 1997.

[8] Francesco Bassi and Stefano Rebay. A high-order accurate discontinuous finite element method for the numerical solution of the compressible Navier-Stokes equations. *Journal of computational physics*, 131(2):267–279, 1997.

[9] Emmanuel Bossy. Evaluation ultrasonore de l'os cortical par transmission axiale: modélisation et expérimentation in vitro et in vivo. 2003.

[10] F Brezzi and LD Marini. Virtual element and discontinuous Galerkin methods. In *Recent developments in discontinuous Galerkin finite element methods for partial differential equations*, pages 209–221. Springer, 2014.

[11] Julien Diaz. Gar6more2D (Analytical solutions of wave propagation problems in stratified media). *https://gforge.inria.fr/projects/gar6more2d/*.

[12] Julien Diaz. Approches analytiques et numériques de problèmes de transmission en propagation d'ondes en régime transitoire. Application au couplage fluide-structure et aux méthodes de couches parfaitement adaptées. 2005.

[13] Guy G. Drijkoningen. Introduction to reflection seismology. *Lecture notes - TA3630*, 2015.

[14] Herbert Egger, Fritz Kretzschmar, Sascha M Schnepp, and Thomas Weiland. A space-time discontinuous galerkin trefftz method for time dependent maxwell's equations. *SIAM Journal on Scientific Computing*, 37(5):B689–B711, 2015.

[15] Charbel Farhat, Isaac Harari, and Ulrich Hetmaniuk. A discontinuous Galerkin method with Lagrange multipliers for the solution of Helmholtz problems in the mid-frequency regime. *Computer Methods in Applied Mechanics and Engineering*, 192(11):1389–1419, 2003.

[16] F FRS. Trefftz type approximation and the generalized finite element method – history and development. *Computer Assisted Mechanics and Engineering Sciences*, 4:305–316, 1997.

[17] Gwénaël Gabard. Discontinuous Galerkin methods with plane waves for time-harmonic problems. *Journal of Computational Physics*, 225(2):1961–1984, 2007.

[18] Ismael Herrera. Trefftz method: a general theory. *Numerical Methods for Partial Differential Equations*, 16(6):561–580, 2000.

[19] Jan S Hesthaven and Tim Warburton. *Nodal discontinuous Galerkin methods: algorithms, analysis, and applications*. Springer Science & Business Media, 2007.

[20] Ralf Hiptmair, Andrea Moiola, and Ilaria Perugia. Plane wave discontinuous Galerkin methods for the 2D Helmholtz equation: analysis of the p-version. *SIAM Journal on Numerical Analysis*, 49(1):264–284, 2011.

[21] Ralf Hiptmair, Andrea Moiola, and Ilaria Perugia. Error analysis of Trefftz-discontinuous Galerkin methods for the time-harmonic Maxwell equations. *Mathematics of Computation*, 82(281):247–268, 2013.

[22] Robert M Kirby, Spencer J Sherwin, and Bernardo Cockburn. To CG or to HDG: a comparative study. *Journal of Scientific Computing*, 51(1):183–212, 2012.

[23] Fritz Kretzschmar, Andrea Moiola, Ilaria Perugia, and Sascha M Schnepp. A priori error analysis of space–time Trefftz discontinuous Galerkin methods for wave problems. *IMA Journal of Numerical Analysis*, 36(4):1599–1635, 2015.

[24] Fritz Kretzschmar, Sascha M Schnepp, Igor Tsukerman, and Thomas Weiland. Discontinuous Galerkin methods with Trefftz approximations. *Journal of Computational and Applied Mathematics*, 270:211–222, 2014.

[25] Patrick Le Tallec. *Modélisation et calcul des milieux continus*. Editions Ecole Polytechnique, 2009.

[26] Artur Macig and Jörg Wauer. Solution of the two-dimensional wave equation by using wave polynomials. *Journal of Engineering Mathematics*, 51(4):339–350, 2005.

[27] P. Antonietti I. Mazzierei. A high-order discontinuous Galerkin approximation to ordinary differential equations with applications to elastodynamics. 2016.

[28] Andrea Moiola, R Hiptmair, and I Perugia. Plane wave approximation of homogeneous Helmholtz solutions. *Zeitschrift für Angewandte Mathematik und Physik (ZAMP)*, 62(5):809–837, 2011.

[29] Andrea Moiola and Ilaria Perugia. A space–time Trefftz discontinuous Galerkin method for the acoustic wave equation in first-order formulation. *Numerische Mathematik*, pages 1–47, 2017.

[30] Steffen Petersen, Charbel Farhat, and Radek Tezaur. A space-time discontinuous Galerkin method for the solution of the wave equation in the time domain. *International journal for numerical methods in engineering*, 78(3):275–295, 2009.

[31] Radek Tezaur and Charbel Farhat. Three-dimensional discontinuous Galerkin elements with plane waves and Lagrange multipliers for the solution of mid-frequency Helmholtz problems. *International journal for numerical methods in engineering*, 66(5):796–815, 2006.

[32] Erich Trefftz. Ein Gegenstuck zum Ritzüschen Verfahren. *Proc. 2nd Int. Cong. Appl. Mech., Zurich, 1926*, pages 131–137, 1926.

[33] Dalei Wang, Radek Tezaur, and Charbel Farhat. A hybrid discontinuous in space and time Galerkin method for wave propagation problems. *International Journal for Numerical Methods in Engineering*, 99(4):263–289, 2014.

[34] Lucas C Wilcox, Georg Stadler, Carsten Burstedde, and Omar Ghattas. A high-order discontinuous Galerkin method for wave propagation through coupled elastic–acoustic media. *Journal of Computational Physics*, 229(24):9373–9396, 2010.

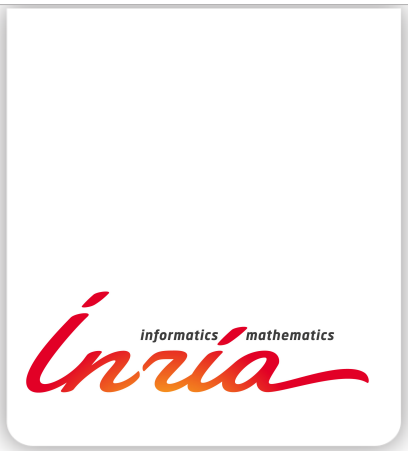

RESEARCH CENTRE
BORDEAUX – SUD-OUEST

200 avenue de la Vieille Tour
33405 Talence Cedex

Publisher
Inria
Domaine de Voluceau - Rocquencourt
BP 105 - 78153 Le Chesnay Cedex
inria.fr

ISSN 0249-6399